Stockholm University

# Bachelor Thesis

Degree Project in
Marine Geology 15 hp

# Stable isotopes and palaeoecology signals in Quaternary planktonic foraminifera from the Arctic Ocean

Bella Dillan

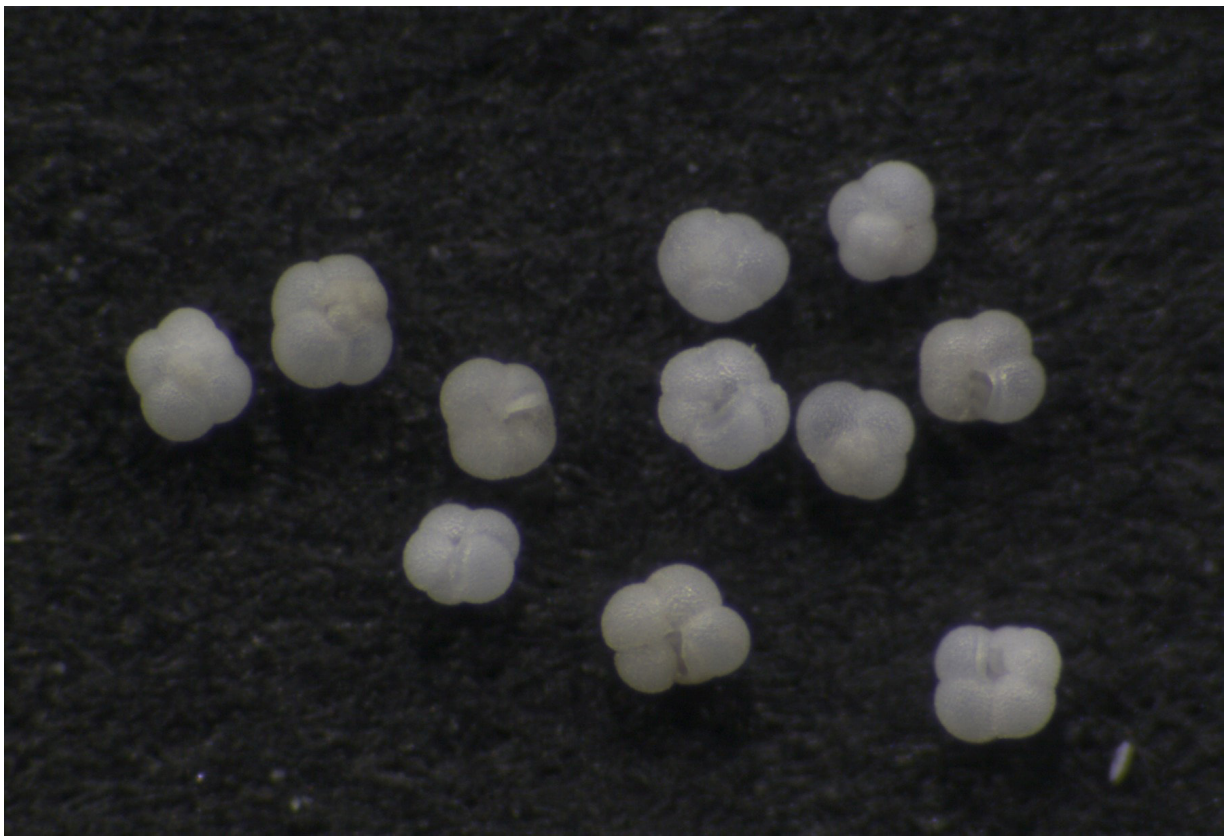

Stockholm 2023

Department of Geological Sciences
Stockholm University
SE-106 91 Stockholm

# Acknowledgements

Firstly, I would like to thank Professor Helen Coxall for giving me this project which has introduced me to the microfossil world and given me a greater understanding of the use and importance of foraminifera within paleoclimate reconstructions. I also want to thank Helen Coxall, Flor Vermassen and Tirza Weitkamp for their guidance through the process of this project. I want to thank Haoyi Yao for helping me at the Sil lab and Ule Ninnemann for the help with the isotope analysis on *T. egelida* and *T. quinqueloba* in Bergen, making it possible for me to use them in this study. Lastly, I want to thank my friends Mikaela Krona and Gustaf Larsson that I could turn to for feedback and also Robert Dunst, Mattias Barkelius, Elise Lindell, Sandra Morawiecki and my family for their support and help. You are great!

## Abstract

The full consequences of the rapidly disappearing sea-ice in the Central Arctic Ocean system are unknown. It is therefore important to learn more about previous interglacials to predict the future. Paleodata from the Central Arctic Ocean is scarce and to be able to make projections of the consequences for global climate change, more research within paleoceanography is needed. A common approach to investigate past ocean conditions is to measure the stable oxygen and carbon isotope ratio ($\delta^{18}O$ and $\delta^{13}C$) in the calcareous fossilised foraminifera shells, which may provide an understanding of e.g. salinity, ocean temperature and sea ice conditions. The aim of this study is to reconstruct the surface water conditions in the Central Arctic Ocean during previous Quaternary interglacials MIS11 and MIS5. By using this approach on known modern Arctic Ocean foraminifera, the paleoecological isotopic signals can be traced into the past. The foraminifera used were planktonic species *N. Pachyderma, T. quinqueloba, T. egelida* and benthic species *C. wuellerstorfi* and *O. tener*. An important difference between the past two interglacials is the presence of *T. egelida* in MIS11 which can not be found in MIS5 or today. A clear $\delta^{13}C$ offset was found in MIS11 between *T. egelida* and *N. pachyderma* while the relationship between *N. pachyderma* and *T. quinqueloba* in MIS5 and the modern period were similar. This could be due to a strong metabolic effect in *T. egelida*.

## Abstrakt

I och med den globala uppvärmningen smälter havsisen i Arktiska havet snabbt bort. Vad konsekvenserna kommer bli för havscirkulationen i centrala Arktis och det globala havssystemet är osäkert. Då det inte finns tillräckligt med paleodata från Arktiska havet krävs därför mycket mer forskning för att kunna förutsäga framtiden. En viktig metod som används för att studera paleooceanografi är att mäta förhållandet av de stabila syre- och kolisotoperna ($\delta^{18}O$ och $\delta^{13}C$) i fossiliserade foraminifera-kalkskal. Detta kan ge en insikt i havsförhållanden såsom salinitet, temperatur och isförhållanden. Syftet med den här studien är att rekonstruera förhållandena av ytvattnet i det Centrala Arktiska havet genom att använda foraminifera under de tidigare interglacialerna MIS11 och MIS5 under kvartär. De arter av foraminifera som användes var planktoniska *N. Pachyderma, T. quinqueloba, T. egelida* och bentiska *C. wuellerstorfi* och *O. tener.* En viktig skillnad mellan de två tidigare interglacialerna är att *T. egelida* endast kan hittas under MIS11. En förskjutning i $\delta^{13}C$ kunde även observeras mellan *T. egelida* under MIS11 och *N. Pachyderma* under MIS5. Detta tros vara på grund av en metabolisk fraktioneringseffekt i *T. egelida*.

Keywords: Paleoclimate, Arctic Ocean, Foraminifera, Pleistocene, paleoecology, palaeoceanography, MIS5, MIS11

# Table of contents

**1. Introduction……..……4**
2. Theoretical background……5
2.1 Arctic foraminifera ……..……5
2.2 Foraminifera test stable isotope fractionation…….……6
2.3 Arctic Oceanography and paleoceanography…….……8
2.4 Glacial and interglacial periods……..10
3. Methods……...11
4. Results……14
5. Discussion……...18
6. Conclusions……22
7. References……...23
8. Appendices……..25

# 1. Introduction

To be able to predict what the full consequences for the rapidly disappearing sea-ice in the Central Arctic Ocean system will be and what impact it will have on the global climate it is necessary to investigate past interglacials, which were also warm periods in the past. One way to do this is by using the unicellular protists foraminifera. Foraminifera can be found throughout marine environments where they dwell in both surface waters (planktonic) or live on the seafloor or at/below the water-sediment contact (benthic). They are widely used in palaeoceanography to reconstruct past oceanic environments such as ocean temperature, salinity, carbon cycling of the past and stratification (Kucera, 2007). This can be made by using the stable oxygen and carbon isotope composition ratios ($\delta^{18}O$ and $\delta^{13}C$) of the calcareous foraminifera shells (also known as tests). Because the tests are assumed to have similar $\delta^{18}O$ and $\delta^{13}C$ as the surrounding seawater where it calcifies they are great tracers of ocean properties and climate changes (Kucera, 2007; Pados *et al.*, 2015). By understanding the controls of oxygen and carbon isotopic ratio in the test, the past ocean-climate conditions can be reconstructed.

Today there are no continuous $\delta^{18}O$ and $\delta^{13}C$ records from the Central Arctic Ocean. Recent work has suggested that the ice loss was extensive based on findings of the subpolar *Turborotalita quinqueloba* (*T. quinqueloba*) during the last interglacial, Marine Isotope Stage 5 (MIS5, ca. 130-80 ka). *T. quinqueloba* which lives in ice-free conditions, does not live in the polar region today. Furthermore, the enigmatic *Turborotalita egelida* (*T. egelida*) could be found during the earlier interglacial, Marine Isotope Stage 11 (MIS11, ca. 424-374 ka). This finding also indicates that conditions during the interglacial periods were different. By analysing the foraminifera composition during MIS5 and MIS11 we can try to find out what the surface water conditions were in the past and how these subpolar species could invade the Arctic Ocean.

In this study a geochemical analysis will be applied using stable oxygen and carbon isotope ratios ($^{18}O/^{16}O$ and $^{13}C/^{12}C$) on foraminifera from the central Arctic Ocean. By using multiple well known species (*Neogloboquadrina pachyderma*, *Cibicidoides wuellerstorfi* and *Oridorsalis tener)* for comparison with *T. quinqueloba* and *T. egelida,* this thesis will try to reconstruct the paleoecology and depth habitat during the previous interglacials MIS5 and MIS11, as well as our current interglacial Holocene.

The aim for this study is to try answering the questions:

- Are the foraminifera species showing different stable isotopic signals than today?
- Can similarities in the $\delta^{18}O$ and $\delta^{13}C$ composition of the locations be observed to find out about ocean properties i.e. water chemistry, surface temperature, salinity and stratification, and/or planktonic foraminiera biology and ecology?
- Is there a difference between *T. quinqueloba* and *T. egelida* that can say something about MIS5 and MIS11?

# 2. Theoretical background

## 2.1 Arctic foraminifera

Today *N. pachyderma* is the most common planktonic foraminifera found in the polar province in the Arctic Ocean. It can be found at/in the Atlantic halocline where they thrive in the cold saline waters (fig 1). Usually *N. pachyderma* are not found in salinities lower than 32 psu (practical salinity unit) and it has recently been found out that they are asymbiotic species, meaning that they do not live in symbiosis with algae (Takagi *et al.*, 2019). The second planktonic foraminifera, *T. quinqueloba,* can today be found in the subpolar regions. It thrives in the warmer ice-free north Atlantic waters with salinities around 33-34.5 psu. *T. quinqueloba* dwells in the shallower near-surface water (Simstich et al., 2003) and are like *N. pachyderma* asymbiotic (Takagi *et al.*, 2019). The presence of *T. quinqueloba* in the Arctic Ocean during the interglacial Marine isotope stage 5 is therefore thought to be due to a stronger and warmer Atlantic water inflow or a different nutrient composition (Werner *et al.*, 2013). *T. egelida* is considered to be a morphotype of *T. quinqueloba*. It could be found during the interglacial MIS11 without the polar *N. pachyderma* derived from cores of the Central Arctic Ocean (O'Regan *et al.*, 2019). Since *T. egelida* is an extinct species much is still not known about it.

The epifaunal *Cibicidoides wuellerstorfi* (*C. wuellerstorfi*) and infaunal *Oridoralis Tener* (*O. tener*) live at depths of the seafloor where the temperature is uniformly low, and are adapted to oligotrophic conditions (Rathmann *et al.*, 2004). Since the epifaunal *C. wuellerstorfi* lives on the seafloor and the infaunal *O. tener* below the sediment-water contact they will trace different physical and biological properties. Today *O. tener* commonly occurs in sea ice covered areas in the central Arctic Ocean (Hanslik, 2011).

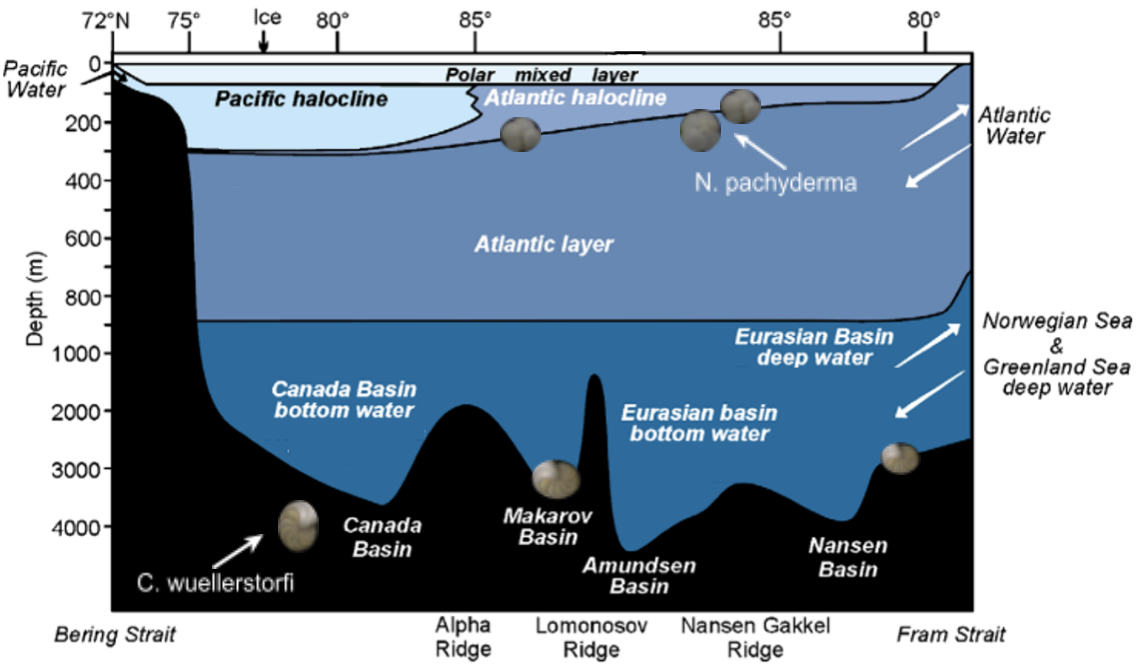

**Figure 1.** Modified cross section of the Central Arctic Ocean showing typical depth habitat of planktonic (*N. pachyderma*) and benthic (*C. wuellerstorfi*) foraminifera and water inflow and outflow (Macdonald et al., 2023).

## 2.2 Foraminifera test stable isotope fractionation

Typically the nutrient composition and carbon dioxide of the water column in the Arctic Ocean increases with depth while the oxygen levels and water temperature decrease (fig 1). Diverse depth habitats of foraminifera can therefore record physical and biological properties through the water. A study by Volkmann and Mensch (2001) has shown that the studied Arctic foraminifera do not calcify in equilibrium with the ambient seawater. The offsets between the equilibrium calcite values had been studied and described as 'vital effects' related to different isotopic uptake in organisms due to their biology compared to equilibrium calcite value by Pados *et al.* (2015).

One vital effect is metabolic activity which discriminates against heavy isotopes of carbon ($^{13}C$). A high metabolic activity is characteristic for small species but also for earlier ontogenetic stages (Birch *et al.*, 2013; Pados *et al.*, 2015). Heavier tests tend to have higher $\delta^{18}O$ and lower $\delta^{13}C$ values (Pados *et al.*, 2015). Unfavourable conditions such as low salinity in freshwater can also lead to vital effects, making the foraminifera grow faster, decreasing $\delta^{18}O$ of their tests (Kucera, 2007). Increased primary production from when the sea ice is melting is another one. The increased primary production can trigger phytoplankton blooms which in turn could increase the pH and carbonate ion concentration hence decrease $\delta^{18}O$ of the tests.

The main regional factor that affects the isotopic composition of the global ocean, thus the $^{18}O/^{16}O$ and $^{13}C/^{12}C$ composition of the test is the ice volume effect (Kucera, 2007) (figure 2). Because sea ice stores a lot of $^{16}O$ an increased temperature would lead to a release of $^{16}O$ back to the ocean when the sea ice is melting. Local changes such as changes in advection and upwelling causes a mix of oxygen isotopes while precipitation causes the local $\delta^{18}O$ to decrease and evaporation the $\delta^{18}O$ to increase (Kucera, 2007).

Global factors affecting the $^{13}C/^{12}C$ composition of the seawater is the release of carbon from the lithosphere and growth of the terrestrial biosphere (figure 3). Carbon uptake of the terrestrial biosphere causes the $\delta^{13}C$ in the atmosphere to increase since most plants discriminate against the heavier isotope when photosynthesizing. Growth of the terrestrial biosphere would hence cause an increase of $\delta^{13}C$ in the ocean. A decrease of the terrestrial biosphere would give the opposite effect, causing the $\delta^{13}C$ in the atmosphere to decrease, hence decreasing the $\delta^{13}C$ of seawater. The main local changes of stable carbon isotope in the seawater are photosynthesis causing $\delta^{13}C$ to increase while respiration causes the $\delta^{13}C$ to decrease, and change is advection/upwelling (Kucera, 2007). An increased pH could also lead to fractionation towards a decreased $\delta^{13}C$ (Pados *et al.*, 2015).

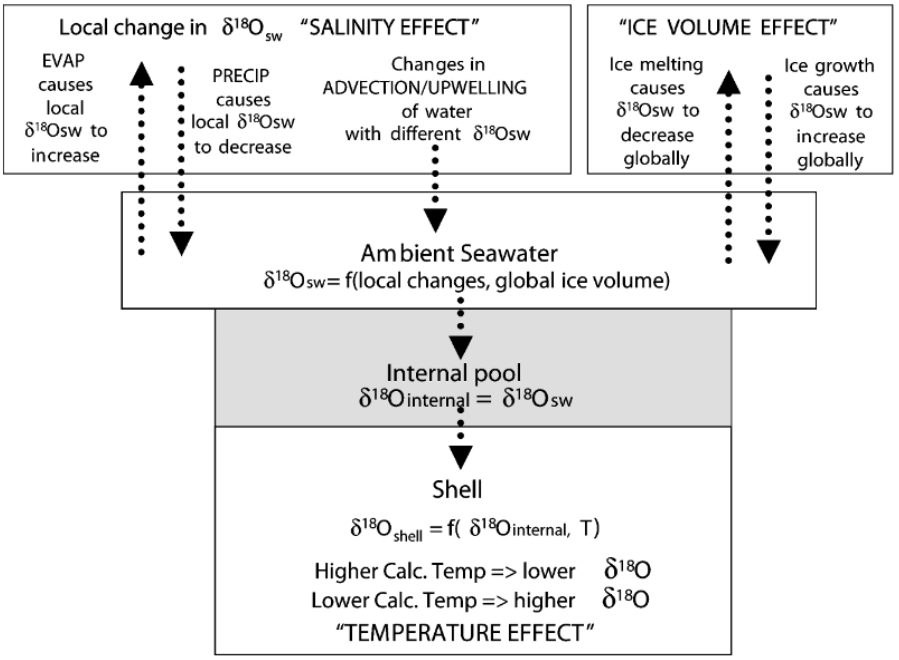


**Figure 2.** Environmental factors affecting the $\delta^{18}O$ of the foraminifera tests (Ravelo and Hillaire-Marcel, 2007).

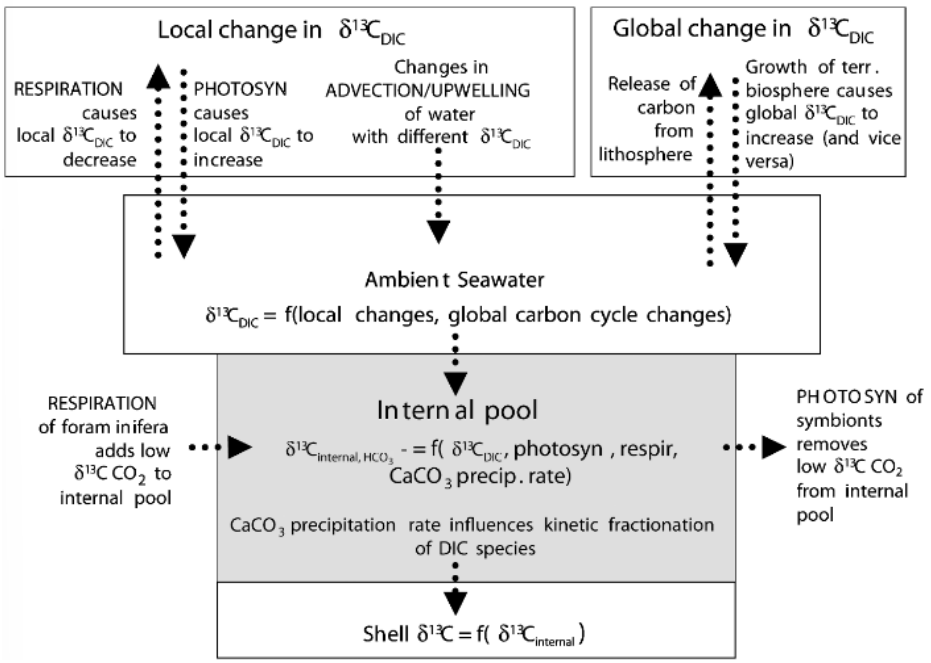


**Figure 3.** Environmental factors affecting the $\delta^{13}C$ of the foraminifera tests (Ravelo and Hillaire-Marcel, 2007).

## 2.3 Arctic oceanography and paleoceanography during Pleistocene

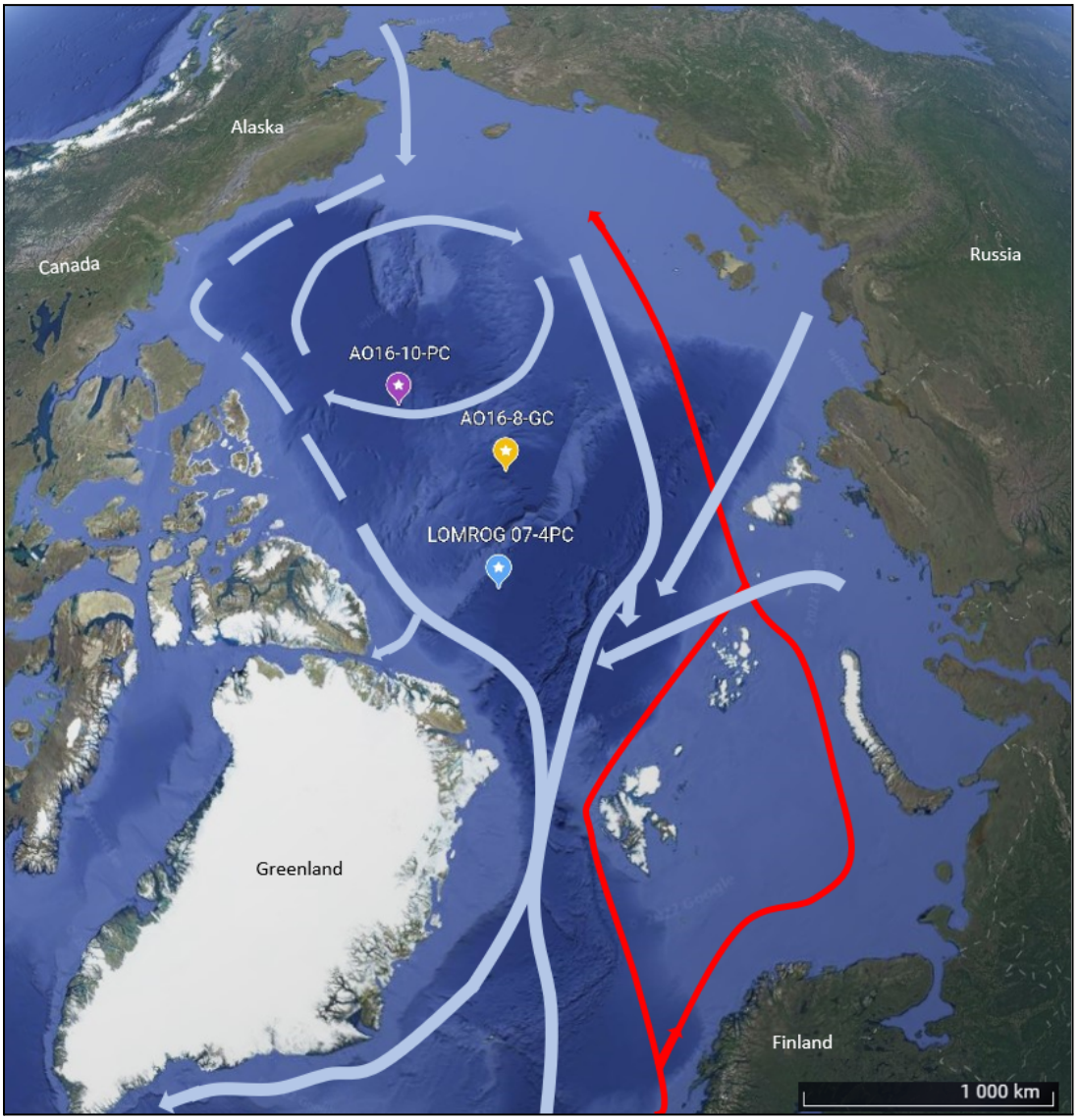


**Figure 4**. Map of the Arctic circle showing the locations of the retrieved cores (LOMROG 07-4PC, AO16-10PC and AO16-8GC), the north Atlantic current (more specific called the Norwegian current in red) and the transpolar current and Beaufort Gyre (blue). The modified map is produced with Google Earth pro. Notice that no north arrow has been added since the study area is in the North Pole.

The study area is located in the Arctic Ocean, north of Canada and Greenland (figure 4). Two major ocean basins are the Amerasian Basin and Eurasian Basin and are separated by the Lomonosov Ridge. Two major currents off the Arctic Ocean circulation are the transpolar and Beaufort Gyre currents. The third major current is the North Atlantic current. The North Atlantic current carries warm and saline water masses northwards into the basins which extends 200-800 m under the Transpolar current. During interglacials a strong intensity of Atlantic water got into the Arctic Ocean called the Atlantification (Werner *et al.,* 2013). The Atlantic water inflow is thought to have carried high productivity and/or high Atlantic water temperatures, resulting in a strong heat flux to the Arctic (Werner *et al.,* 2013). The transpolar

current carries cold and fresh polar waters from the Arctic ocean southwards (Pados *et al.*, 2015). The Arctic Ocean also gets inflow water from the northern Atlantic through the Canadian archipelagos via Baffin Bay and from the Pacific Ocean through the Bering Strait (Hanslik, 2011). Consequently, inflow of nutrients from the Pacific surface water and Atlantic water enrich the Atlantic Ocean (Rennermalm *et al.*, 2007; Hanslik, 2011).

The surface temperature of the Arctic Ocean is generally around -1.5 to -1 °C and gets gradually warmer through the first 500 m of the water column. At 500 m depth, reaching 1 °C the temperature starts decreasing until 1500 m depth where the temperature stays constant around -1 to -0.5 °C (figure 5). The salinity of the Arctic surface water is around 30 to 32 psu (practical salinity unit) and gradually increases to 35 psu at 450-500 m depth where it remains more or less constant through the water column (Rennermalm *et al.*, 2007).

Today, much of the Arctic Ocean is one of the least productive parts of the world's Oceans, due to the sea ice cover (Hanslik, 2011). The sea ice extent is at least fifteen percent during September and forms during winter when the weather is cooler and reaches its maximum extent in March (Molar-Candanosa, 2022). In general the ice drift follows the surface circulation characterised by the Beaufort Gyre and Transpolar Drift (Hanslik, 2011).

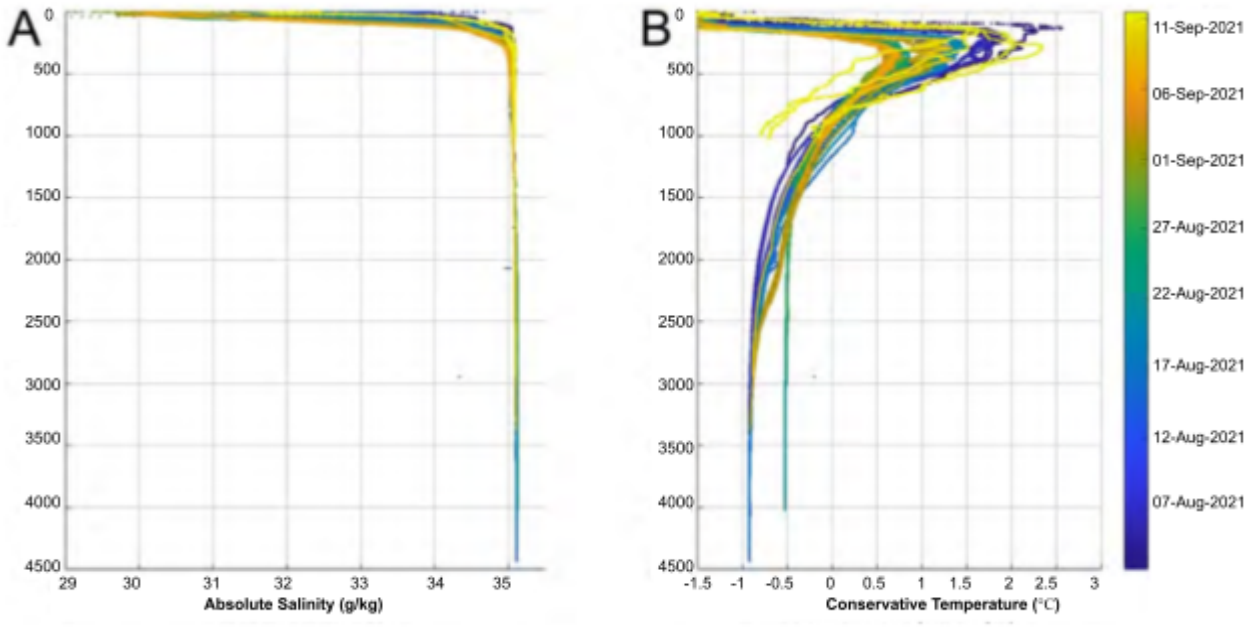


**Figure 5.** Salinity (A) and conservative temperature (B) from vertical profiles of CTD data north of Greenland (Snoeijs-Leijonmalm, 2021).

## 2.4 Glacial and interglacial periods

Glacial periods are defined as periods with growing ice sheets and times with retreating ice sheets as interglacial periods (National Oceanic and Atmospheric Administration [NOAA], 2021). The glacial-interglacial cycles are caused by variations in the Earth's orbit through time also known as the Milankovitch cycles (Marshak, 2015) which causes a change in the amount of radiation that the Earth receives. Periods with more intensive solar radiation will lead to retreating ice sheets while periods with less intensive solar radiation will lead to growing ice sheets (National Oceanic and Atmospheric Administration [NOAA], 2021). By using benthic $\delta^{18}O$ stack the glacial-intercycles can be traced throughout the Quaternary period (fig. 6) (Lisiecki and Raymo, 2005). The high $\delta^{18}O$ represents the glacial periods and the decreasing $\delta^{18}O$ the interglacial periods. It is important to know that foraminifera in the Central Arctic Ocean do not occur during glacial periods which is why there is no separate stable isotope curve for local dating during these periods. For each site a separate age model was developed by other workers (table 1), this is however outside the scope of this thesis.

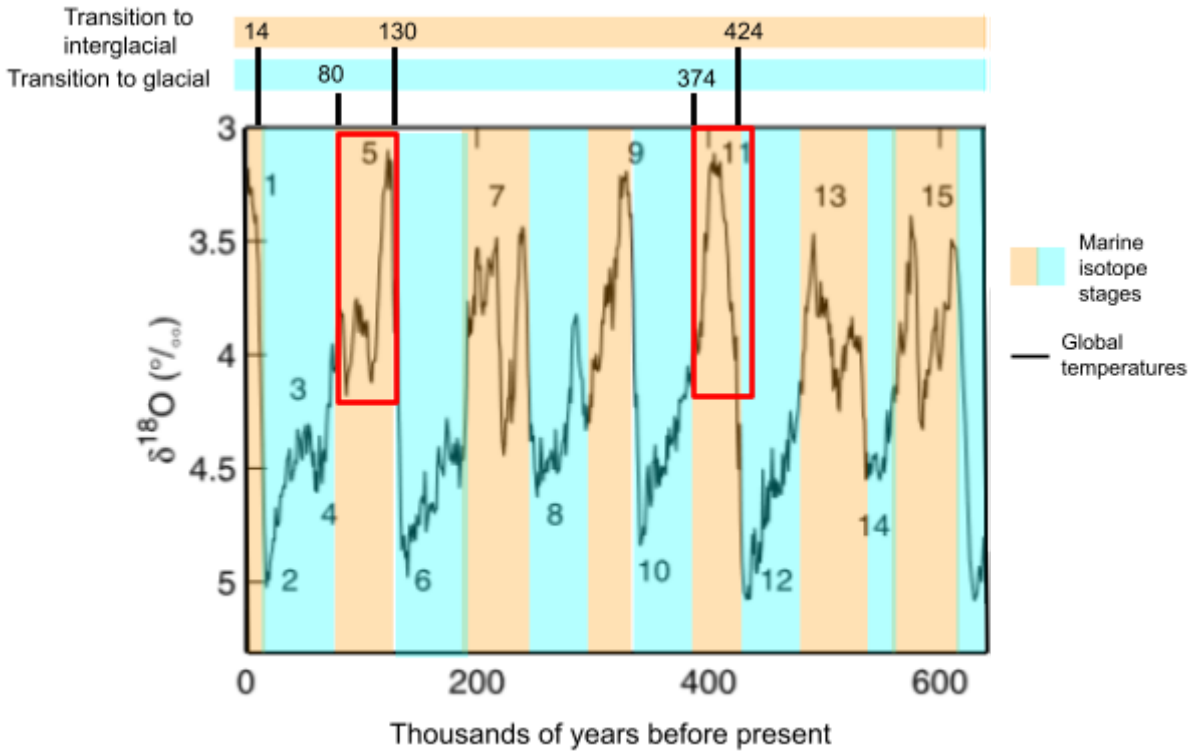


**Figure 6.** Modified benthic $\delta^{18}O$ stack from Lisiecki and Raymo (2005) showing the global temperature (black line) from thousands of years before present to recent time. The interglacials are presented in orange and glacials in blue. The interglacials MIS11 and MIS5 are marked in red boxes.

## 3. Methods

The samples were collected from two expeditions with Icebreaker Oden in the Arctic Ocean; expedition LOMROG07 in 2007 (Lomonosov Ridge off Greenland) and expedition AO16 in 2016 (Arctic Ocean in 2016). The sediment cores LOMROG07-4PC (86.70117° N, 53.76717° W, 5.49m length), AO16-8-GC (86.7795° N, 140.6433° W, 3.59m length) and AO16-10-PC (82.398° N, 141.245° W, 7.96m length) were retrieved from a water depth of 2.620 m, 2.872m and 811m (table 1). From each of the three cores a sample from modern age (core-top sample), MIS5 and MIS11 were taken to be analysed. The species of foraminifera used for each period are shown in table 2. The samples had been wet-sieved with a >63-µm sieve before the study.

**Table 1.** Cores used in this study. For sample details see Appendix A.

| Core name | Latitude | Longitude | Water depth (m) | Core length (m) | Age model |
|---|---|---|---|---|---|
| AO16-8-GC | 86.7795° N | 140.6433° W | 2620 | 3.59m | Vermassen et al. (2021) |
| AO16-10-PC | 82.398° N | 141.245° W | 2872 | 7.96 | F. Vermassen (personal communication) |
| LOMROG07-4PC | 86.70117° N | 53.76717° W | 811 | 5.49 | Vermassen et al. (2021) |

**Table 2.** Species representing the modern, MIS5 and MIS11 age for each core.

| Age | Species |
|---|---|
| Modern | *N. pachyderma,*<br>*C. wuellerstorfi, O. tener* |
| MIS5 | *N. pachyderma, T. quinqueloba,*<br>*C. wuellerstorfi, O. tener* |
| MIS11 | *T. egelida, C. wuellerstorfi, O. tener* |

In order to avoid an influence of ontogenetic isotope fractionation effects on the isotopic results, samples were dry-sieved before picking (Hillaire-Marcel et al., 2004). *N. pachyderma* were picked from the 150-250 µm fraction, *T. quinqueloba* and *T. egelida* from the 63-125µm fraction and *C. wuellerstorfi* and *O. tener* from the 63-250µm fraction due to little material. Planktonic and benthic taxonomy followed Young et al. (2017). Each sample analysis was repeated twice with a weight of 0.20 mg except for *T. egelida* and *T. quinqueloba* that had a minimum weight of 0.034 mg, respectively. Altogether 54 benthic and planktonic foraminifera samples were collected for analysis; 21 of these, containing the *T .egelida* and *T. quinqueloba* specimens including 2 test samples, were sent off to the Farlab at the University of Bergen, Norway due to their low weight which could not be analysed in Stockholm. The rest were analysed at the department of Geological Sciences, Stockholm University.

For the samples analysed at Stockholm university, the picked samples were put in marked vials. A 0.2 mg standard isotope based on the Vienna Pee Dee Belemnite (VPDB) together with 0.2 mg of the in-house working standard $CaCO_3$-Merck was prepared in separate vials for every sixteenth sample. The samples were put in the oven at $50^{\circ}C$ for 12 hours and then flushed with helium for 10 minutes to avoid contamination from the air. 100 µl of over 99% sulfuric acid was added in the samples to react with the foraminifera to produce $CO_2$. Lastly, samples were put in a MAT 253 mass spectrometer connected to a gasbench II device to measure the oxygen and carbon isotopes. Stable carbon and oxygen isotope ratios are expressed against the VPDB standard, following equations (1) and (2). The working standard, $CaCO_3$-*Merck* along with two international standards IAEA-CO-1 and NBS 18 were analysed each day interspersed with samples. The external precision for the samples between 200 - 300 µg was better than 0.102‰ for $\delta^{18}O$ and 0.068‰ for $\delta^{13}C$, based on the long-term reproducibility (1σ SD) of the working standard $CaCO_3$-*Merck.* No drift correction for the machine was used.

$$\delta^{13}\mathbf{C}\ ‰ = \left( \frac{\left(\frac{^{13}C}{^{12}C}\right)_{Sample}}{\left(\frac{^{13}C}{^{12}C}\right)_{Standard}} - 1 \right) \times 1000‰ \qquad (1)$$

$$\delta^{18}\mathbf{O}\ ‰ = \left( \frac{\left(\frac{^{18}O}{^{16}O}\right)_{Sample}}{\left(\frac{^{18}O}{^{16}O}\right)_{Standard}} - 1 \right) \times 1000‰ \qquad (2)$$

For stable isotope analyses in Bergen, a Finnigan MAT253 mass spectrometer with an online Kiel IV was used. The values were reported on a Vienna Pee Dee Belemnite (VPDB) scale where two working standards (CM12 and Riedel) along with two international standards (NBS-18 and NBS-19) were analysed each day interspersed with samples. The external precision for the samples sent to Bergen was between 10 and 100 µg and was better than 0.08 ‰ and 0.04 ‰ for $\delta^{18}O$ and $\delta^{13}C$, respectively. The long-term reproducibility (1σ SD) of the working standard was based on CM12.

Results will be presented in stable isotope cross plots shown in figure 7 where $\delta^{18}O$ values are represented on the y-axis and $\delta^{13}C$ values on the x-axis. The interpretation will broadly follow the model shown in figures 7 and 8.

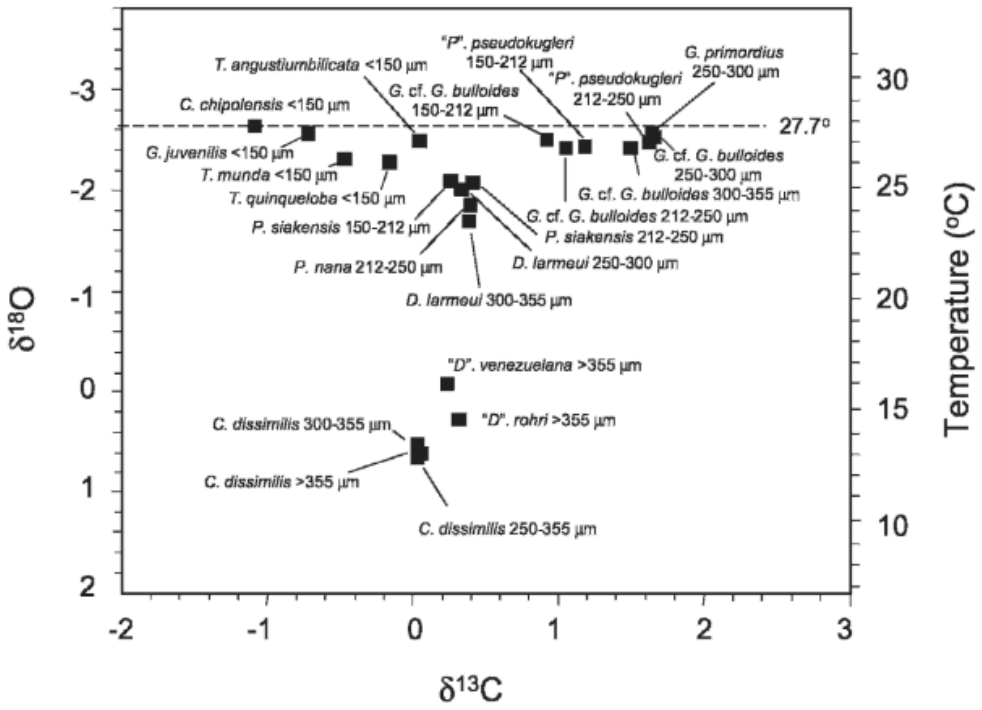


**Figure 7.** Example of a $\delta^{18}O$ and $\delta^{13}C$ cross plot of foraminifera in units per mil (Pearson and Wade., 2009).

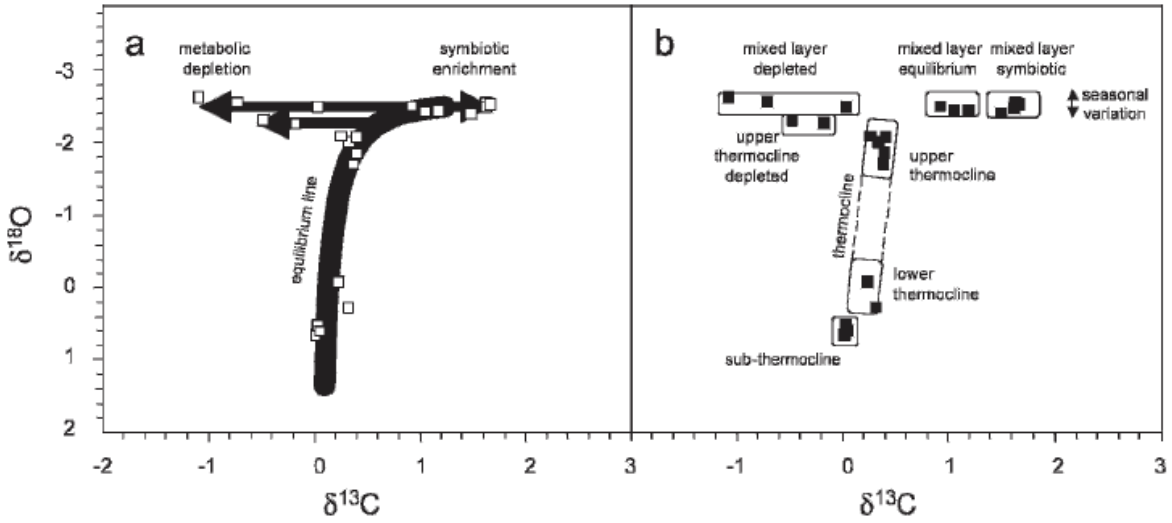


**Figure 8.** Interpretation model of $\delta^{18}O$ and $\delta^{13}C$ for the data from figure 7. **a** Isotopic $\delta^{13}C$ signals around zero are at the equilibrium line with dissolved inorganic carbon while lower or higher values are in the metabolic depletion or symbiotic enrichment areas. **b** Foraminifera different ecological niches based on their stable isotope values (Pearson and Wade, 2009).

# 4. Results

Results show microscope images of the well preserved foraminifera and stable isotope analysis presented in a series of $\delta^{18}O$ and $\delta^{13}C$ cross plots. The main aim is to compare the stable isotope signatures of planktonic species from the surface ocean. The results are following an interpretive model by Pearson and Wade (2009) from lower latitudes (figure 8) it is therefore important to note that other factors in the Arctic Ocean such as meltwater also influence the seawater chemistry. The data are compared to studies by Pados et al. (2015) from the Fram Strait and Simstich et al., (2003) from the Nordic Seas.

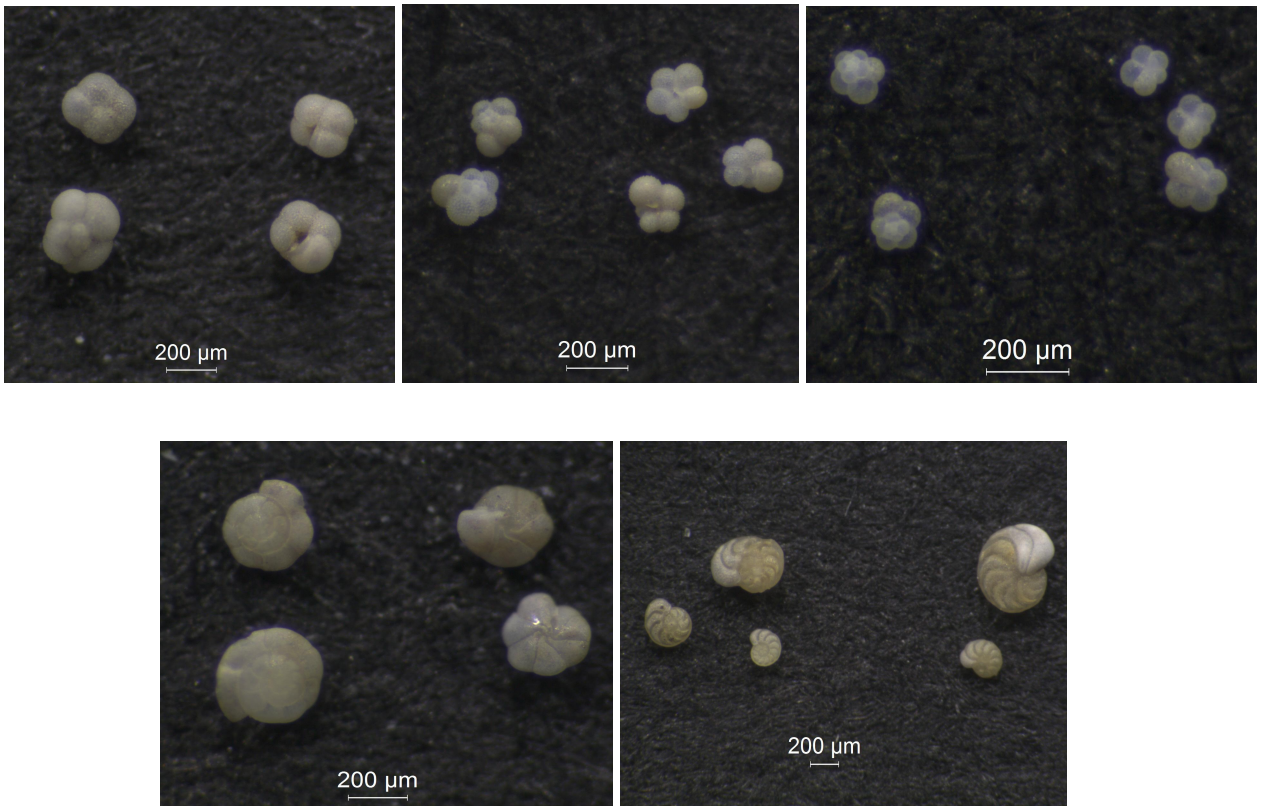


**Figure 9.** Images of the ventral (left) and dorsal side (right) of the planktonic and benthic foraminifera collected for this study. Starting on the upper left image is *Neogloboquadrina pachyderma* from AO16-8GC, MIS5, *Turborotalita egelida* from AO16-10PC, MIS11, *Turborotalita quinqueloba* picked from LOMROG07, MIS5, *Oridorsalis tener* from AO16-8GC, Modern period and *Cibicidoides wuellerstorfi* from AO16-8GC, MIS11.

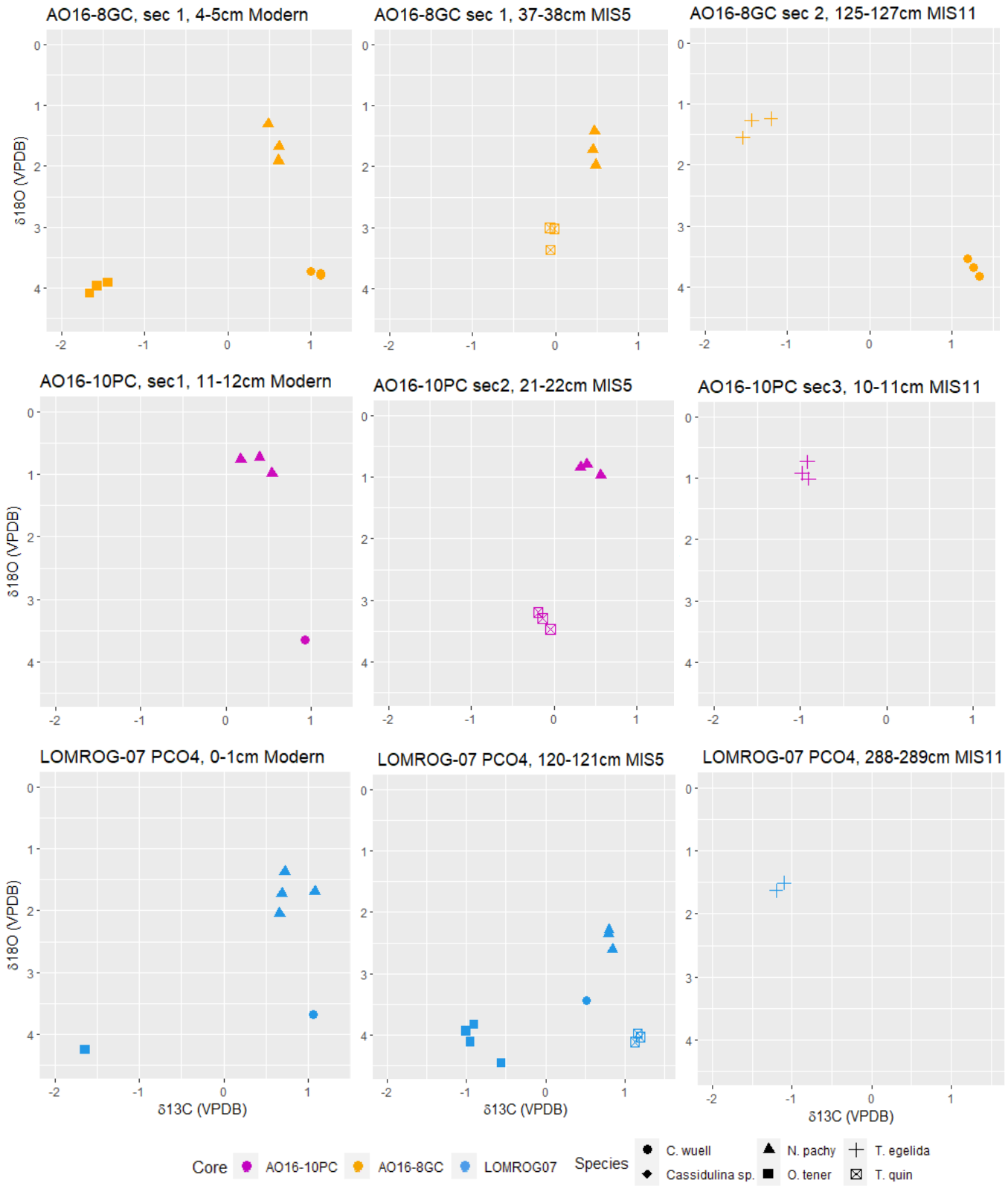


**Figure 10.** $\delta^{18}O$ and $\delta^{13}C$ values of *N. pachyderma* (triangle), *C. wuellerstorfi* (circle), *T. quinqueloba* (crossed square), *T. egelida* (cross) and *O. tener* (square) shown in scatter plots produced with Rstudio for the individual sites. The colours represent three different cores starting with AO16-8GC (yellow points) at the top, AO16-10PC (pink points) in the middle and LOMROG07-PC04 (blue points) at the bottom. Horizontally for each core, the plots are ordered by increasing sample age,

starting from 'modern' on the left towards the older MIS5 in the middle and MIS11 to the right. Missing values are because of too little material (see appendix B).

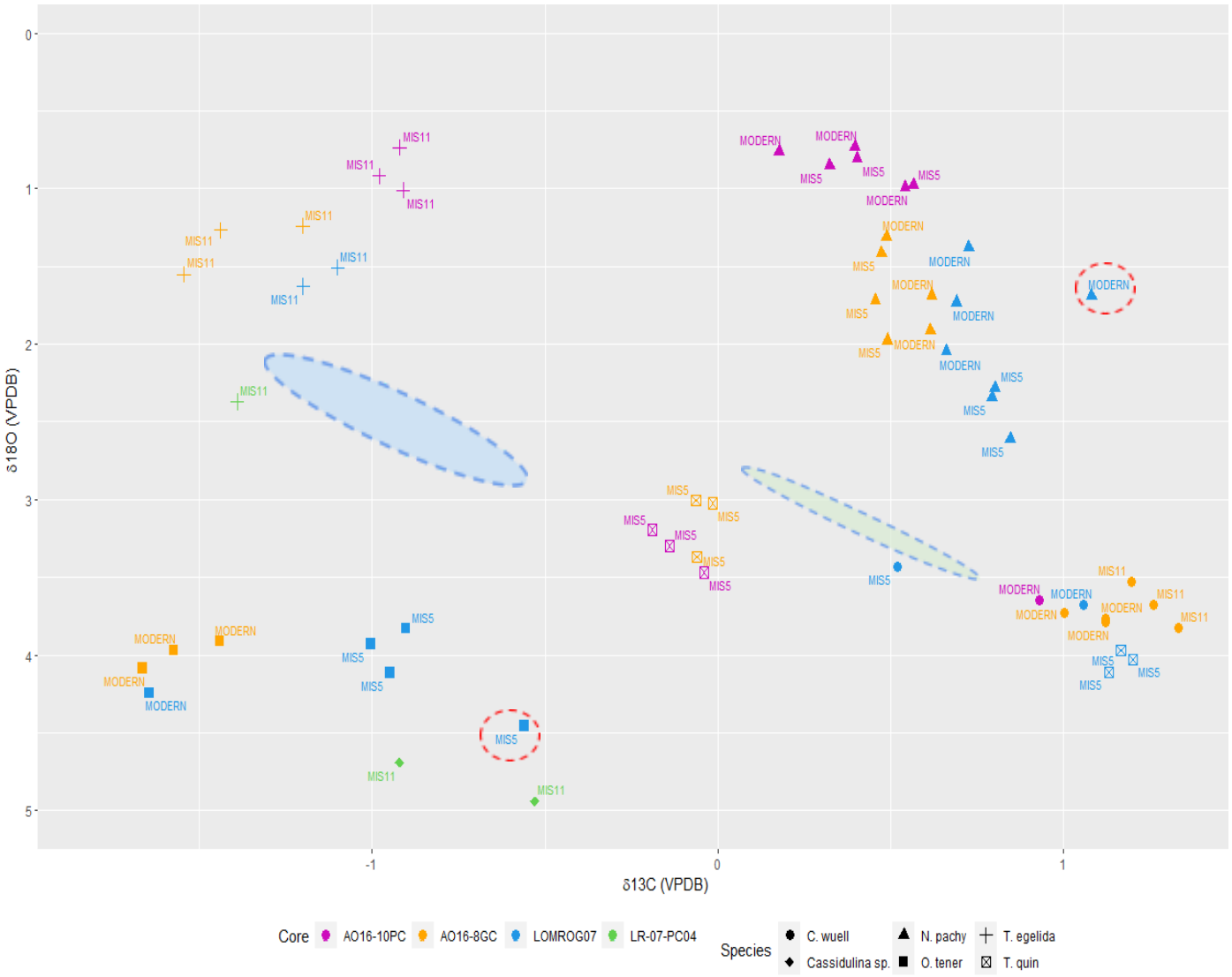


**Figure 11.** Scatterplot of all $\delta^{18}O$ and $\delta^{13}C$ data for modern, MIS5 and MIS11 age. *N. pachyderma, C. wuellerstorfi, T. quinqueloba, T. Egelida* and *O. tener* (shown with different point shapes). *Cassidulina sp.* (diamond shape) and *T. egelida* from a MIS11 sample from core LR-07-PCO4 (Green) have been added for data comparison. Note that LOMROG07 and LR-07-PC04 are the same core. Samples marked with red circles are 'check samples' that were analysed in both Bergen and at IGV. Blue and green ellipses are added for data comparison and represent the proximate isotopic fields for modern sedimented *T. quinqueloba* and *N. pachyderma* respectively from Fram Strait (Pados et al., 2015) (see figure 12).

All scatterplots show a clear difference between the isotopic composition of benthic and planktonic species. Comparing the check samples from Bergen with the samples from the Sil lab the check samples gives a higher $\delta^{13}C$ value by ca. 0.25‰. The results of *N. pachyderma* show similar $\delta^{13}C$ values as Pados et al. (2015) in figure 11 and 12, ranging from 1.08‰ to 0.39‰, while the $\delta^{18}O$ composition from this study shows a much lower value ranging from 0.73‰ to 2.61‰. Location AO16-10PC for *N. pachyderma* show similar $\delta^{18}O$ values for the modern age and MIS5 but different $\delta^{13}C$ values. *N. pachyderma* for location AO16-8GC and

LOMROG07 however show different $\delta^{18}O$ values for modern age and MIS5 but similar $\delta^{13}C$ values. *T. quinqueloba* show higher values for both the $\delta^{13}C$ and $\delta^{18}O$ compared to Pados et al. (2015). The $\delta^{13}C$ values for core AO16-8GC and AO16-10PC range between -0.19 ‰ to -0.04 ‰ and core LOMROG-07 PCO4 from 1.2 ‰ to 1.13‰ showing approximately 1‰ difference from the other two locations. The $\delta^{18}O$ values for *T. quinqueloba* is between 3.00 ‰ and 3.46‰ for core AO16-8GC and AO16-10PC and 3.97‰ to 4.11‰ for LOMROG-07 PCO4. It is worth noting that the MIS5 $\delta^{18}O$ for *N. pachyderma* and *T. quinqueloba* are different even though they are from the same core location. However there seems to be a more or less consistent difference between MIS5 for *T. quinqueloba* and *N. pachyderma* for each of the locations.

*T. egelida* show general low values of $\delta^{13}C$ and $\delta^{18}O$ ranging from -1.54‰ to -0.91‰ and 0.73‰ to 1.63‰, respectively. Here it is worth pointing out the similar $\delta^{18}O$ values between *T. egelida* and *N. pachyderma*. Compared to *T. egelida* from LR-07-PCO4 (green), core AO16-8GC and LOMROG07 seem to have similar negative $\delta^{13}C$ value trend ranging from -1.54‰ to -1.1‰, but lower $\delta^{18}O$ values ranging from 1.24‰ to 1.63‰. *T. egelida* from core AO16-10PC shows a higher value of $\delta^{13}C$ ranging from -0.98‰ to -0.91‰ and lower $\delta^{18}O$ values ranging from 0.73‰ to 1.00‰.

Values of *C. wuellerstorfi* show general high $\delta^{13}C$ and $\delta^{18}O$ composition. $\delta^{13}C$ starting from 0.92‰ to 1.33‰ and $\delta^{18}O$ from 3.52‰ to 3.82‰. The modern age *C. wuellerstorf*i have similar $\delta^{18}O$ values but slightly different $\delta^{13}C$ values compared to MIS11 which seem to have an decreasing $\delta^{18}O$ and $\delta^{13}C$ value. One extreme value from MIS5 LOMROG07 shows a lower delta carbon value of 0.51 ‰. *O. tener* show a general low $\delta^{13}C$ value, -1.66‰ to -0.56‰ especially for the modern age compared to MIS5 and MIS11 (represented by *Cassidulina sp.*). The $\delta^{18}O$ value for *O. tener* is high ranging from 3.82‰ to 4.45‰.

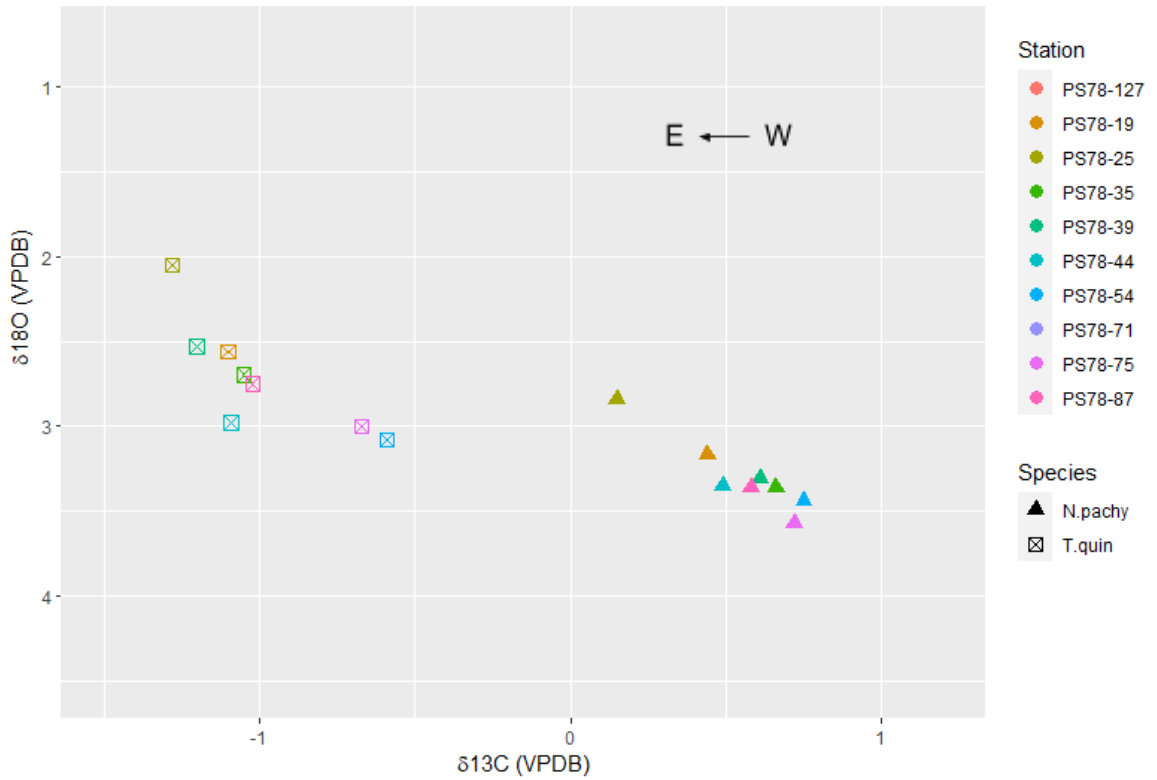


**Figure 12.** $\delta^{18}O$ and $\delta^{13}C$ values of *N. pachyderma* and *T. quinqueloba* from surface sediment samples (modern age) at 10 stations (coloured points) along an E-W transect in the Fram strait (Pados et al., 2015).

# 5. Discussion

As mentioned before, the scatter plots show a clear difference between the isotopic composition of benthic and planktonic species which is expected due to their large different living habitat. The check samples from Bergen seem to give a higher $\delta^{13}C$ value compared to the SIL lab. A possible explanation for this could be that no drift correction for the SIL lab machine was used and/or that the sample sizes for the two labs were different. However, since the approach used to correct data by the Bergen lab is not known it is uncertain. Starting with *N. pachyderma* which compared to Pados et al. (2015) show much lower $\delta^{18}O$ range. Whether this is due to different size fractionation of foraminifera, different water masses with different temperature and chemistry or vital effects is uncertain. Since it is known today that *N. pachyderma* are asymbiotic a depletion of $\delta^{18}O$ due to higher carbon dioxide fixation caused by photosynthesis is excluded. For the MIS11 and MIS5 samples, another factor for the low $\delta^{18}O$ compared to Pados et al. (2015) could be the difference in age. Different interglacial periods may have had different water masses, ocean temperature and chemistry compared to the modern interglacial. Also the foraminifera analysed for the modern period in this study is from a different location and could be older than the surface samples analysed in the study by Pados et al. (2015). However, more research on *N. pachyderma* from these locations and periods would be needed to see if a similar trend can be seen.

*N. pachyderma* from location AO16-10PC show the lowest $\delta^{18}O$ values where similar $\delta^{18}O$ composition between MIS5 and the modern period can be observed. The similar $\delta^{18}O$ values suggest that there was no significant change in water condition such as surface salinity and temperature during the periods. A possible explanation for the lower $\delta^{18}O$ composition at AO16-10PC could be due to changes in advection/upwelling of water with different $\delta^{18}O$ (Kucera, 2007). Another possibility that could explain why AO16-10PC has the lowest $\delta^{18}O$ values could be due to an increased primary production from when the sea ice is melting, triggering phytoplankton blooms. This would later increase the pH and the carbonate ion concentration and thus lead to a decrease $\delta^{18}O$ of the tests. An increased primary production could however not explain the lower $\delta^{13}C$ values. The low scattered $\delta^{13}C$ values of AO16-10PC from modern age and MIS5 might nonetheless be explained by changes in advection/upwelling of water with lighter $^{12}C$ values.

Looking at the data from AO16-8GC, MIS5 and the modern period show scattered values indicating that there may have been changes such as advection/upwelling or depth ecology of the foraminifera within the interglacials at this location. The slightly higher $\delta^{18}O$ values compared to AO16-10PC indicate that *N. pachyderma* lived slightly deeper in the surface water with less fresh water and higher $\delta^{18}O$. This location could also have had a slightly increased salinity leading to favourable conditions for the specie not to grow faster, increasing the $\delta^{18}O$ of the test. Interestingly, AO16-8GC shows similar $\delta^{13}C$ values during MIS5 and more or less during the modern age. This indicates similar water mass carbon chemistry during the two different ages where the modern time had slightly higher values than MIS5. An increased $\delta^{13}C$ for this location close to the sea surface is assumed to be caused by a higher primary production, especially during MIS5. Same things discussed for location AO16-8GC can have affected *N. pachyderma* at location LOMROG07 except that the effects were even stronger giving higher $\delta^{18}O$ and $\delta^{13}C$ values. However, here the factors affecting $\delta^{13}C$ seemed to be stronger during the modern age compared to MIS5 in contrast to AO16-8GC, and the $\delta^{18}O$ stronger during MIS5.

Since not much is known about the enigmatic *T. egelida* it is difficult to interpret the factors affecting their isotope values. Interestingly, even though N. pachyderma are abundant today in the Arctic Ocean and during MIS5 there are none during MIS11. However it is clear that *T. egelida* shows similar $\delta^{18}O$ compared to MIS5 and modern *N. pachyderma* during MIS11. The similar $\delta^{18}O$ indicates that *T. egelida* most likely lived at similar shallow water depth as *N. pachyderma*. The different $\delta^{13}C$ composition could indicate that the primary production during MIS11 was generally low, or the surface waters were affected by a source of $^{12}C$-enriched water or due to a strong biological carbon vital effect. A vital effect that could explain the low $\delta^{13}C$ composition is the metabolic fractionation whereby respired carbon, rich in $^{12}C$, as described by Birch *et al.* (2013), gets preferentially incorporated into the test. Considering that no other planktic species could be found with *T. egelida* during MIS11 (appendix B) the Arctic Ocean conditions might also have been so different that other species did not thrive.

Looking at location AO16-10PC *T. egelida* has clustered $\delta^{13}C$ values around -0.91‰ to -0.98‰ while core AO16-8GC show a linear decreasing $\delta^{13}C$ pattern which could indicate that there were local changes at this location during MIS11. Since LOMROG07- PC04 is missing a sample measurement it is unclear if the $\delta^{13}C$ values also are decreasing in a linear pattern or are roughly clustered. The *T. egelida* from AO16-8GC, shows one of the lowest $\delta^{13}C$ among all the analysed *T. egelida*. This could indicate that AO16-8GC surface waters were most impacted by $^{12}C$-enriched water and AO16-10PC least (fig. 11). However, more isotope analysis would be needed to explore this pattern or if there is a high variability in $\delta^{13}C$ and $\delta^{18}O$ values.

Considering that the subpolar *T. quinqueloba* most likely ended up in the Arctic ocean due to the Atlantic current reaching further in to the Arctic ocean the high $\delta^{18}O$ values compared to *N. pachyderma* during MIS5, particularly in LOMROG07 are unexpected. A similar offset between *T. quinqueloba* and *N. pachyderma* for core AO16-8GC and AO16-10PC can be seen in the study by Pados (2015) on modern age planktic foraminifera. However, for the Pados study *T. quinqueloba* samples are showing a generally low $\delta^{18}O$ composition compared to *N. pachyderma*. Although, looking at the two western most stations from the Pados study where the transpolar current is situated *T. quinqueloba* show slightly higher $\delta^{18}O$ values. Contrary to the study by Pados, Simstich et al. (2003) study has shown that in the East Greenland transpolar current *N. pachyderma* is found at slightly shallower depths compared to *T. quinqueloba.* Why *N. pachyderma* seems to prefer the shallower water depth and *T. quinqueloba* the slightly deeper part is unclear. One possibility is that *N. pachyderma* is more adaptable to its Arctic environment than *T. quinqueloba*. Another reason for the low $\delta^{18}O$ composition of *T. quinqueloba* could be due to the fragile tests leading to fast calcification.

*T. quinqueloba* shows low $\delta^{13}C$ values for core AO16-10PC and AO16-8GC while core LOMROG07 shows very high $\delta^{13}C$ values. Considering that planktic foraminifera usually have $\delta^{13}C$ close to sea water composition and therefore similar $\delta^{13}C$ values the $\delta^{13}C$ compositions for *T. quinqueloba* are surprising. For the high values in core station LOMROG07, it seems like the $\delta^{13}C$ compositions during MIS5 in general are high which could be due to a higher primary production and/or changes in mixture of water masses. However, having values that are more similar to the benthic species *C. wuellerstorfi* is uncommon and are probably due to a distinct vital effect. Core sites AO16-8-GC and AO16-10PC show low $\delta^{13}C$ compositions compared to *N. pachyderm*a. The same offset can be observed in the study by Pados (2015). This could be explained by a metabolic fractionation effect described by Birch et al. (2013).

The modern age $\delta^{18}O$ composition of *C. wuellerstorfi* in AO16-8GC seems to be generally higher than both AO16-10PC and LOMROG07 implying a slightly cooler bottom water mass at that location during modern age. However, only one sample each of modern age *C. wuellerstorfi* could be collected from AO16-10PC and LOMROG07 since the sample species were too few and therefore not sufficient for comparison. Likewise for the single MIS5 isotope analysis obtained from LOMROG07-04 showing lower $\delta^{18}O$ composition which could indicate a warmer ocean bottom. Looking at the $\delta^{18}O$ values during MIS11 from core location

AO16-8GC the values are showing a positive linear pattern where two of the sample repeats are showing slightly lower values. The same pattern could also be observed in *T. egelida* during MIS11 at the same core location. Whether there are short term changes during MIS11 causing this difference at core location AO16-8GC is unclear.

The $\delta^{13}C$ composition in *C. wuellerstorfi* is generally high and compared with Belanger et al. (1981) study in the Norwegian-Greenland sea, it seems to be consistent. The $\delta^{13}C$ composition at core location AO16-8GC during MIS11 varies in a positive linear pattern while the $\delta^{13}C$ composition of the modern age seems to be clustered around the same values. The increasing linear pattern from MIS11 can be due to the different ontogenetic stages since no size range was used for *C. wuellerstorfi*. However, since the reversed linear pattern can be seen for *T. egelida* during MIS11 at the same core station the size fractionation might not be the cause. However there could be local short term effects causing changes during MIS11. A short term effect causing the linear pattern could be due to differences in primary production during MIS11. The similar modern age values for core location AO16-10PC, LOMROG07 and AO16-8GC indicate similar conditions at these sites during modern time. Although core location AO16-10PC shows a slightly lower value which could be caused by either a change in the advection/upwelling of water with different $\delta^{13}C$ composition or lower primary production. As mentioned earlier, the single samples are however not sufficient for comparison nor interpretations.

The infaunal *O. tener* in core LOMROG07 and AO16-8GC shows similar to slightly higher $\delta^{18}O$ composition compared to *C. wuellerstorfi*. This can also be observed in the study by Belanger et al. (1981) explained to be caused by lower pH by Ravelo and Hillaire-Marcel (2007). The one isotope analysis of the modern age *O. tener* in core LOMROG07 show slightly higher $\delta^{18}O$ values compared to the modern age values in core AO16-8GC. This could indicate a slightly cooler habitat under the sediment-water contact during the modern age. However more data of modern age *O. tener* in core LOMROG07-04 is needed for an accurate interpretation. The $\delta^{18}O$ values of the modern age and MIS5 are similar, indicating similar temperature below the sediment-water at these ages and two locations. The added *Cassidulina sp.* from MIS11 in core LOMROG07-04 are showing higher $\delta^{18}O$ values which could indicate cooler temperatures within the sediment surface during MIS11. However it is uncertain if the $\delta^{18}O$ during MIS11 would show similar $\delta^{18}O$ values for *O. tener* considering that they are different species. To explore this more measurements on *O. tener* during MIS11 would be needed.

The $\delta^{13}C$ values are consistent with the values in Belanger et al. (1981) study for the infaunal *O. tener* showing a general low $\delta^{13}C$ composition. Belanger et al. (1981) suggests that taxa with negative $\delta^{13}C$ values live in oxygen-free conditions within sediments which could explain the lower $\delta^{13}C$ values. However, the modern age *O. tener* is showing lower $\delta^{13}C$ values than observed in Belanger et al. (1981) study. This might be because *O. tener* is living within the shallower sediment part that is not completely oxygen-free which could explain the higher $\delta^{13}C$ values during MIS5. A period with low to oxygen-free conditions or that *O. tener*

lived slightly deeper in the sediment might therefore also explain the lower $\delta^{13}C$ values during the modern age. It is worth noting that the study by Belanger et al. (1981) showed that *O. tener* do not have a systematic relationship of $\delta^{13}C$ and $\delta^{18}O$ to bottom water and are therefore not reliable.

## 6. Conclusions

This study presents the first multi-site comparison during our current interglacial Holocene and past interglacials MIS11 and MIS5, using stable isotope compositions ($\delta^{18}O$ and $\delta^{13}C$) of Central Arctic foraminifera. This study also includes the first isotopic data on the enigmatic species *T. egelida.* The $\delta^{18}O$ composition of *N. pachyderma* in MIS5 shows similar values to *T. egelida* in MIS11 indicating similar surface water temperatures during the two interglacials. The close $\delta^{18}O$ values of *T. egelida* and *N. Pachyderma* also suggests that *T. egelida* could live in the cold surface/subsurface fresh water. *T. quinqueloba* in MIS5 show significantly high $\delta^{13}C$ composition compared to *T. quinqueloba* in the Fram Strait which could be due to a strong primary production during MIS5, potentially from a limited sea ice cover, increasing $\delta^{13}C$. It could also be due to changes in mixture of water masses during MIS5. The much lower $\delta^{13}C$ composition of *T. egelida* compared to *N. pachyderma* is thought to be due to a strong metabolic fractionation effect, although it may alternatively be due to a source of $^{12}C$-enriched water. Further research would be needed on *C. wuellerstorfi* for better bottom water interpretations.

# 7. References


Belanger, P.E., Curry, W.B. and Matthews, R.K. (1981) 'Core-top evaluation of benthic foraminiferal isotopic ratios for paleo-oceanographic interpretations', *Palaeogeography, Palaeoclimatology, Palaeoecology*, 33(1), pp. 205–220. Available at: https://doi.org/10.1016/0031-0182(81)90039-0.

Birch, H. *et al.* (2013) 'Planktonic foraminifera stable isotopes and water column structure: Disentangling ecological signals', *Marine Micropaleontology*, 101, pp. 127–145. Available at: https://doi.org/10.1016/j.marmicro.2013.02.002.

Flor Vermassen, Matt O'Regan, Gabriel West, Thomas M. Cronin & Helen K. Coxall (2021) Testing the stratigraphic consistency of Pleistocene microfossil bioevents identified on the Alpha and Lomonosov Ridges, Arctic Ocean, Arctic, Antarctic, and Alpine Research, 53:1, 309-323. Available at: https://doi.org/10.1080/15230430.2021.1988356

Hanslik, D. (2011) 'Late Quaternary Biostratigraphy and Paleoceanography of the Central Arctic Ocean' (No. 345) [Doctoral dissertation, Department of Geological Sciences, Stockholm University], p. 42. ISBN: 978-91-7447-311-7.

Kucera, M. (2007) 'Chapter Six Planktonic Foraminifera as Tracers of Past Oceanic Environments', in *Developments in Marine Geology*. Elsevier, pp. 213–262. Available at: https://doi.org/10.1016/S1572-5480(07)01011-1.

Macdonald, R.W., Harner, T. and Fyfe, J. (2023) 'Recent climate change in the Canadian Arctic and its impact on contaminant pathways', *Science of the Total Environment*, 342, pp. 5–86. Doi:10.1016/j.scitotenv.2004.12.059.

Marshak, S. (2015). Earth: Portrait of a Planet: 5th International student Edition. WW Norton & Company.

Molar-Candanosa, R. (2022) *2022 Arctic Summer Sea Ice Tied for 10th-Lowest on Record*, *NASA*. Available at: http://www.nasa.gov/feature/esnt/2022/2022-arctic-summer-sea-ice-tied-for-10th-lowest-on-record (Accessed: 10 November 2022).

National Oceanic and Atmospheric Administration. (2021, October). *Glacial-Interglacial Cycles*. Available at: NOAA National Environmental Satellite, Data, and Information Service: Glacial-Interglacial Cycles

O'Regan, M. *et al.* (2019) 'Stratigraphic Occurrences of Sub-Polar Planktic Foraminifera in Pleistocene Sediments on the Lomonosov Ridge, Arctic Ocean', *Frontiers in Earth Science*, 7. Available at: https://www.frontiersin.org/articles/10.3389/feart.2019.00071 (Accessed: 6 January 2023).

Pados, T. *et al.* (2015) 'Oxygen and carbon isotope composition of modern planktic foraminifera and near-surface waters in the Fram Strait (Arctic Ocean) – a case study', *Biogeosciences*, 12(6), pp. 1733–1752. Available at: https://doi.org/10.5194/bg-12-1733-2015.

Pearson, P.N. *et al.* (2001) 'Warm tropical sea surface temperatures in the Late Cretaceous and Eocene epochs', *NATURE -LONDON-*, 1 January, pp. 481–487. ISSN: 0028-0836.

Rathmann, S. *et al.* (2004) 'Mg/Ca ratios of the benthic foraminifera Oridorsalis umbonatus obtained by laser ablation from core top sediments: Relationship to bottom water temperature', *Geochemistry, Geophysics, Geosystems*, 5(12). Available at: https://doi.org/10.1029/2004GC000808.

Ravelo, A.C. and Hillaire-Marcel, C. (2007) 'Chapter Eighteen The Use of Oxygen and Carbon Isotopes of Foraminifera in Paleoceanography', in *Developments in Marine Geology*. Elsevier, pp. 735–764. Available at: https://doi.org/10.1016/S1572-5480(07)01023-8.

Rennermalm, A.K. *et al.* (2007) 'Relative sensitivity of the Atlantic meridional overturning circulation to river discharge into Hudson Bay and the Arctic Ocean', *Journal of Geophysical Research: Biogeosciences*, 112(G4). Available at: https://doi.org/10.1029/2006JG000330.

Simstich, J., Sarnthein, M. and Erlenkeuser, H. (2003) 'Paired δ18O signals of Neogloboquadrina pachyderma (s) and Turborotalita quinqueloba show thermal stratification structure in Nordic Seas', *Marine Micropaleontology*, 48(1), pp. 107–125. Available at: https://doi.org/10.1016/S0377-8398(02)00165-2.

Snoeijs-Leijonmalm, P. and the SAS-Oden 2021 Scientific Party (2022). Expedition Report SWEDARCTIC Synoptic Arctic Survey 2021 with icebreaker Oden. Swedish Polar Research Secretariat. 300 pp.

Takagi, H. *et al.* (2019) 'Characterizing photosymbiosis in modern planktonic foraminifera', *Biogeosciences*, 16(17), pp. 3377–3396. Available at: https://doi.org/10.5194/bg-16-3377-2019.

Volkmann, R. and Mensch, M. (2001) 'Stable isotope composition (d 18O, d 13C) of living planktic foraminifers in the outer Laptev Sea and the Fram Strait', *Marine Micropaleontology*, p. 26.

Werner, K. *et al.* (2013) 'Atlantic Water advection versus sea-ice advances in the eastern Fram Strait during the last 9 ka: Multiproxy evidence for a two-phase Holocene', *Paleoceanography*, 28(2), pp. 283–295. Available at: https://doi.org/10.1002/palo.20028.

Young, J.R., Wade, B.S., & Huber B.T. (eds) '*Streptochilus*' pforams@mikrotax website. 21 Apr. 2017.

URL:http://www.mikrotax.org/pforams/index.php?taxon=Streptochilus&module=pf_cenozoic

# 8. Appendices

## Appendix A: Analysed data of foraminifera

Table A1: Data of foraminifera stable carbon and oxygen isotope composition and information of the species size fraction, core sample and depth, number of species picked and place of analysis.

| Bella sample ID | Isotope sample nr: | | Repeat-code | Core sample: | Species: | Size fraction: | No of individuals: | Mass: | Age: | Place of analyses: | δ13C vs VPDB, ‰ | δ18O vs VPDB, ‰ |
|---|---|---|---|---|---|---|---|---|---|---|---|---|
| Bella_11 | 11 | Slide 11 | R1 | AO-16-8-GC sec 1, 37-38cm | T.quin | 63>150 | 140 | 34 µg | MIS5 | Bergen, Norway | -0,02 | 3,02 |
| Bella_13 | 13 | Slide 13 | R2 | AO-16-8-GC sec 1, 37-38cm | T.quin | 63>150 | 140 | 75 µg | MIS5 | Bergen, Norway | -0,06 | 3,00 |
| Bella_15 | 15 | Slide 15 | R3 | AO-16-8-GC sec 1, 37-38cm | T.quin | 63>150 | 140 | 62 µg | MIS5 | Bergen, Norway | -0,06 | 3,37 |
| Bella_12 | 12 | | R2 | AO-16-8-GC sec 1, 37-38cm | N.pachy | 150>250 | 51 | 250µg | MIS5 | SIL lab, SU | 0,46 | 1,72 |
| Bella_14 | 14 | | R3 | AO-16-8-GC sec 1, 37-38cm | N.pachy | 150>250 | 47 | 240µg | MIS5 | SIL lab, SU | 0,47 | 1,42 |
| Bella_10 | 10 | | R1 | AO-16-8-GC, sec 1, 37-38cm | N.pachy | 150>250 | 48 | 230µg | MIS5 | SIL lab, SU | 0,49 | 1,98 |
| Bella_17 | 17 | Slide 17 | R1 | AO-16-8-GC sec 2, 125-127cm | T.egelida | 63>150 | 110 | 59 µg | MIS11 | Bergen, Norway | -1,20 | 1,24 |
| Bella_19 | 19 | Slide 19 | R2 | AO-16-8-GC sec 2, 125-127cm | T.egelida | 63>150 | 110 | 32 µg | MIS11 | Bergen, Norway | -1,44 | 1,27 |
| Bella_21 | 21 | Slide 21 | R3 | AO-16-8-GC sec 2, 125-127cm | T.egelida | 63>150 | 110 | 61 µg | MIS11 | Bergen, Norway | -1,54 | 1,55 |
| Bella_18 | 18 | | R2 | AO-16-8-GC sec 2, 125-127cm | C.wuell | 63>250 | 9 | 200µg | MIS11 | SIL lab, SU | 1,26 | 3,67 |
| Bella_20 | 20 | | R3 | AO-16-8-GC sec 2, 125-127cm | C.wuell | 63>250 | 12 | 240µg | MIS11 | SIL lab, SU | 1,33 | 3,82 |
| Bella_16 | 16 | | R1 | AO-16-8-GC, sec 2, 125-127cm | C.wuell | 63>250 | 11 | 210µg | MIS11 | SIL lab, SU | 1,20 | 3,53 |
| Bella_1 | 1 | | R1 | AO-16-8-GC, sec 1, 4-5cm | N.pachy | 150>250 | 45 | 230µg | Modern | SIL lab, SU | 0,62 | 1,69 |
| Bella_2 | 2 | | R1 | AO-16-8-GC, sec 1, 4-5cm | C.wuell | 63>250 | 4 | 210µg | Modern | SIL lab, SU | 1,00 | 3,73 |
| Bella_3 | 3 | | R1 | AO-16-8-GC, sec 1, 4-5cm | O.umbo/Tener? | 63>250 | approx. 40 | 180µg | Modern | SIL lab, SU | -1,66 | 4,09 |
| Bella_4 | 4 | | R2 | AO-16-8-GC, sec 1, 4-5cm | N.pachy | 150>250 | 45 | 240µg | Modern | SIL lab, SU | 0,61 | 1,91 |
| Bella_5 | 5 | | R2 | AO-16-8-GC, sec 1, 4-5cm | C.wuell | 63>250 | 8 | 230µg | Modern | SIL lab, SU | 1,12 | 3,79 |
| Bella_6 | 6 | | R2 | AO-16-8-GC, sec 1, 4-5cm | O.umbo/Tener? | 63>250 | approx.40 | 230µg | Modern | SIL lab, SU | -1,44 | 3,91 |
| Bella_7 | 7 | | R3 | AO-16-8-GC, sec 1, 4-5cm | N.pachy | 150>250 | 45 | 250µg | Modern | SIL lab, SU | 0,49 | 1,31 |
| Bella_8 | 8 | | R3 | AO-16-8-GC, sec 1, 4-5cm | C.wuell | 63>250 | 4 | 210µg | Modern | SIL lab, SU | 1,12 | 3,76 |
| Bella_9 | 9 | | R3 | AO-16-8-GC, sec 1, 4-5cm | O.umbo/Tener? | 63>250 | approx. 40 | 180µg | Modern | SIL lab, SU | -1,57 | 3,97 |
| Bella_44 | 44 | Slide 44 | R1 | AO16-10PC sec2, 21-22cm | T.quin | 63>150 | 155 | 60 µg | MIS5 | Bergen, Norway | -0,04 | 3,47 |
| Bella_46 | 46 | Slide 46 | R2 | AO16-10PC sec2, 21-22cm | T.quin | 63>150 | 155 | 72 µg | MIS5 | Bergen, Norway | -0,14 | 3,30 |
| Bella_48 | 48 | Slide 48 | R3 | AO16-10PC sec2, 21-22cm | T.quin | 63>150 | 155 | 92 µg | MIS5 | Bergen, Norway | -0,19 | 3,19 |
| Bella_45 | 45 | | R1 | AO16-10PC sec2, 21-22cm | N.pachy | 150>250 | 50 | 219µg | MIS5 | SIL lab, SU | 0,56 | 0,98 |
| Bella_47 | 47 | | R2 | AO16-10PC sec2, 21-22cm | N.pachy | 150>250 | 50 | 240µg | MIS5 | SIL lab, SU | 0,40 | 0,80 |
| Bella_49 | 49 | | R3 | AO16-10PC sec2, 21-22cm | N.pachy | 150>250 | 50 | 214µg | MIS5 | SIL lab, SU | 0,32 | 0,85 |
| Bella_50 | 50 | Slide 50 | R1 | AO16-10PC sec3, 10-11cm | T.egelida | 63>150 | 125 | 121 µg | MIS11 | Bergen, Norway | -0,01 | 1,01 |
| Bella_51 | 51 | Slide 51 | R2 | AO16-10PC sec3, 10-11cm | T.egelida | 63>150 | 125 | 105 µg | MIS11 | Bergen, Norway | -0,98 | 0,92 |
| Bella_52 | 52 | Slide 52 | R3 | AO16-10PC sec3, 10-11cm | T.egelida | 63>150 | 125 | 141 µg | MIS11 | Bergen, Norway | -0,92 | 0,74 |
| Bella_40 | 40 | | R1 | AO16-10PC, sec1 , 11-12cm | N.pachy | 150>250 | 50 | 261µg | Modern | SIL lab, SU | 0,40 | 0,73 |
| Bella_41 | 41 | | R1 | AO16-10PC, sec1 , 11-12cm | C.wuell | 63>250 | 4 | 1510µg | Modern | SIL lab, SU | 0,93 | 3,65 |
| Bella_42 | 42 | | R2 | AO16-10PC, sec1 , 11-12cm | N.pachy | 150>250 | 50 | 270µg | Modern | SIL lab, SU | 0,18 | 0,76 |
| Bella_43 | 43 | | R3 | AO16-10PC, sec1 , 11-12cm | N.pachy | 150>250 | 50 | 213µg | Modern | SIL lab, SU | 0,54 | 0,99 |
| Bella_22 | 22 | | R1 | LOMROG 07 PCO4, 0-1 cm | N.pachy | 150>250 | 66 | 2230µg | Modern | SIL lab, SU | 0,66 | 2,05 |
| Bella_23 | 23 | | R1 | LOMROG 07 PCO4, 0-1 cm | C.wuell | 63>250 | 6 | 202µg | Modern | SIL lab, SU | 1,06 | 3,67 |
| Bella_24 | 24 | | R1 | LOMROG 07 PCO4, 0-1 cm | O.umbo/Tener? | 63>250 | 40 | 220µg | Modern | SIL lab, SU | -1,64 | 4,24 |
| Bella_25 | 25 | | R2 | LOMROG 07 PCO4, 0-1 cm | N.pachy | 150>250 | 48 | 250µg | Modern | SIL lab, SU | 0,69 | 1,73 |
| Bella_26 | 26 | | R3 | LOMROG 07 PCO4, 0-1 cm | N.pachy | 150>250 | 48 | 270µg | Modern | SIL lab, SU | 0,72 | 1,38 |
| Bella_53 | 53 | Slide 53 | R4 | LOMROG07 PCO4, 0-1 cm | N.pachy | 150>250 | 18 | 140 µg | Modern | Bergen, Norway | 1,08 | 1,69 |
| Bella_29 | 29 | Slide 29 | R1 | LOMROG 07 PCO4, 120-121cm | T.quin | 63>150 | 155 | 42 µg | MIS5 | Bergen, Norway | 1,13 | 4,11 |
| Bella_32 | 32 | Slide 32 | R2 | LOMROG 07 PCO4, 120-121cm | T.quin | 63>150 | 155 | 51 µg | MIS5 | Bergen, Norway | 1,2 | 4,03 |
| Bella_35 | 35 | Slide 35 | R3 | LOMROG 07 PCO4, 120-121cm | T.quin | 63>150 | 165 | 50 µg | MIS5 | Bergen, Norway | 1,17 | 3,97 |
| Bella_27 | 27 | | R1 | LOMROG 07 PCO4, 120-121cm | C.wuell | 63>250 | 5 | 143µg | MIS5 | SIL lab, SU | 0,52 | 3,43 |
| Bella_28 | 28 | | R1 | LOMROG 07 PCO4, 120-121cm | N.pachy | 150>250 | 45 | 239µg | MIS5 | SIL lab, SU | 0,85 | 2,61 |
| Bella_30 | 30 | | R1 | LOMROG 07 PCO4, 120-121cm | O.umbo/Tener? | 63>250 | approx. 50 | 249µg | MIS5 | SIL lab, SU | -0,95 | 4,11 |
| Bella_31 | 31 | | R2 | LOMROG 07 PCO4, 120-121cm | N.pachy | 150>250 | 45 | 240µg | MIS5 | SIL lab, SU | 0,80 | 2,28 |
| Bella_33 | 33 | | R2 | LOMROG 07 PCO4, 120-121cm | O.umbo/Tener? | 63>250 | approx. 60 | 250µg | MIS5 | SIL lab, SU | -0,90 | 3,83 |
| Bella_34 | 34 | | R3 | LOMROG 07 PCO4, 120-121cm | N.pachy | 150>250 | 45 | 240µg | MIS5 | SIL lab, SU | 0,79 | 2,35 |
| Bella_36 | 36 | | R3 | LOMROG 07 PCO4, 120-121cm | O.umbo/Tener? | 63>250 | approx. 60 | 220µg | MIS5 | SIL lab, SU | -1,00 | 3,93 |
| Bella_54 | 54 | Slide 54 | R4 | LOMROG07 PCO4 120-121cm | O.umbo/Tener? | 63>150 | 34 | 157 µg | MIS5 | Bergen, Norway | -0,56 | 4,46 |
| Bella_37 | 37 | Slide 37 | R1 | LOMROG 07 PCO4, 288-289cm | T.egelida | 63>150 | 125 | 100 µg | MIS11 | Bergen, Norway | -1,10 | 1,51 |
| Bella_38 | 38 | Slide 38 | R2 | LOMROG 07 PCO4, 288-289cm | T.egelida | 63>150 | 125 | 58 µg | MIS11 | Bergen, Norway | -1,20 | 1,63 |
| Bella_39 | 39 | Slide 39 | R3 | LOMROG 07 PCO4, 288-289cm | T.egelida | 63>150 | 125 | 59 µg | MIS11 | Bergen, Norway | | |

Appendix B: Microscope lab notations of foraminifera.

Figure B1: Notations of foraminifera physical properties and other observations found in each core and age during the microscope lab.

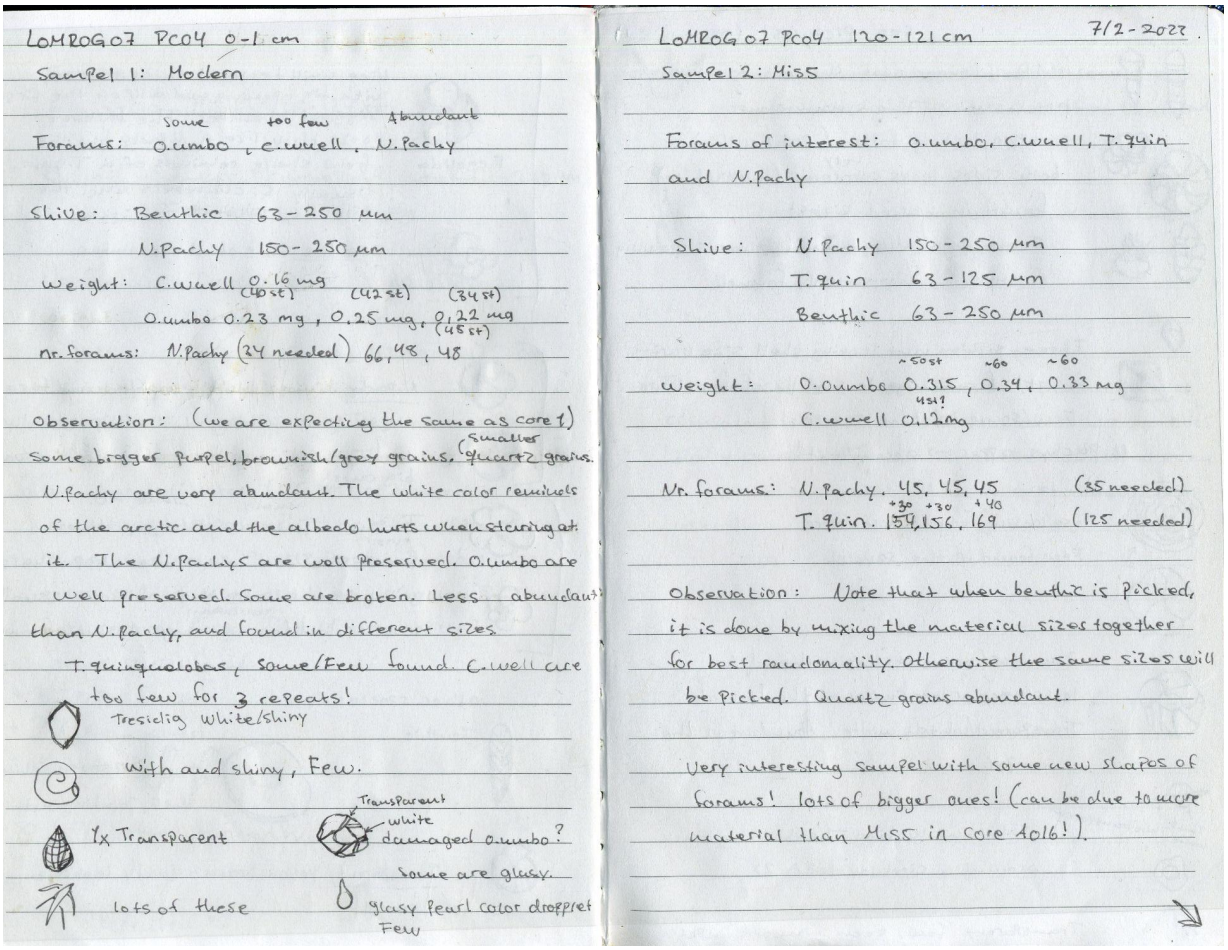

LOMROG07 PC04 0-1 cm
Sample 1: Modern

Forams: some O.umbo, too few C.wuell, Abundant N.Pachy

Shive: Benthic 63-250 µm
N.Pachy 150-250 µm

Weight: C.wuell 0.16 mg (40 st) (42 st) (34 st)
O.umbo 0.23 mg, 0.25 mg, 0.22 mg (45 st)

Nr. forams: N.Pachy (24 needed) 66, 48, 48

Observation: (we are expecting the same as core 1)
some bigger pupel, brownish/grey grains. (smaller quartz grains.
N.Pachy are very abundant. The white color reminds of the arctic and the albedo hurts when staring at it. The N.Pachys are well preserved. O.umbo are well preserved. Some are broken. Less abundant than N.Pachy, and found in different sizes.
T. quinqueloba, some/Few found. C.well are too few for 3 repeats!
Tresiclig white/shiny
with and shiny, Few.
Transparent white damaged o.umbo?
1x Transparent
Some are glasy.
lots of these
glasy pearl color droppret Few

LOMROG07 PC04 120-121 cm 7/2-2022
Sample 2: MIS5

Forams of interest: O.umbo, C.wuell, T.quin and N.Pachy

Shive: N.Pachy 150-250 µm
T.quin 63-125 µm
Benthic 63-250 µm

Weight: O.umbo ~50 st 0.315 (45 st?), ~60 0.34, ~60 0.33 mg
C.wuell 0.12mg

Nr. forams: N.Pachy. 45, 45, 45 (35 needed)
T. quin. 154 (+30), 156 (+30), 169 (+40) (125 needed)

Observation: Note that when benthic is picked, it is done by mixing the material sizes together for best randomality. Otherwise the same sizes will be picked. Quartz grains abundant.

Very interesting sample with some new shapes of forams! lots of bigger ones! (can be due to more material than MIS5 in core 1016!).

See pictures! (Dödetalle bild)

White. Longer and shorter ones. Stripped is not usuall on the smaller ones.

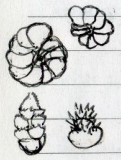

Pumpkin looking foram (prob. benthic) on very both sides looks calcareous (thick white), found in varied sizes!

Reminds of dragonfruit! Upwards growing crystals. Commonly found.

Three-sidden nut looking shell. Size varies a lot! from huge to small. White colour. Few/some in the sampel.

N. pachys appear → abundant!

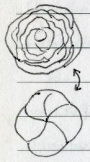

Rose looking foram. White colore. Few found in the sampel.

Rounder/non outsticking head. looks more or less similar on tha backside. Transparent/whitish midle. Abundant in the sampel.







Saturnus looking. The thin ring stuck around a circular ball. 2X



Transparent few, seen in most sampels.

The roundish droped shaped balls seems to have spines! This one had three transparent ones. Few

Looks like a unicorn horn! Small and Large some found

The O.oubo are very abundant in this sampel compared to for the A016-S-GC one where benthics hardly could be found. C. wuellerstorfi is not seen much in this sampel. N. Pachy are abundant as usuall.

LOMROG 07 PC04 288-289 cm 9/2-2022

Sampel 3: MIS II

Forams: T. egelida C. well O. umbo

Shive: T. egelida 63-125 µm

Benthic 63-250 µm

Weight: — (Might have to redo! contaminated.)

nr forams.: T. egelida (95 needed), 125, 175, 175 (+30 +30 +30)

O. umbo Too few

C. well None found

Observation: The material in the sampel look golden/glittery colored in general. The T. egelids are abundant but also longer braided spicies. smaller white quartz grains are abundant.

The Picked T. egelidas will have the golden colour on them They are more transparent in colour than T. egelida in A016-8-GC. Big egelida has a big abacus while the smaller ones has a smaller, on the side on the bigest chamber.

» But the ones without colour or less will be picked. some forams has bits of goldish lumps on them.

Transparent
Abundant.

Braided, usually transparent
Abundant

x1 x1 x1

Saturn looking ball
Few x2

Transparent
some

3 circules on top of each other!
Few x2-3

Few

Few

Few x1

9/2 to
See pictures. 14/2-2022
Repeated x3!
Used to be exchanged to an uncontaminated!

20/1-2022

Sample 1:

A016-8-GC Modern 4.5cm Sec 1 0.025m

N-Pachy Shive: 150 - 250 µm 250 - 63 Benthic

weight: C. well 1: 0.18 mg 2. 0.22 3. 0.21 mg

O. umbo 1: 0.22 mg 2: 0.22 3: 0.22 mg

Nr. of forams: N. Pachy 45, 45, 45

observation: N. Pachyderma are abundant! some yellow and glassy mineral grains (quartz). Few bigger light colored grains. easy to pick N. Pachy!

Benthic types Cibicidoides wuellerstorfi and ordidorsalis umbonatus were randomly picked later on (26/1-2022) C. well are few while O. umbo are abundant.

Repeated 3 times.

oridorsalis Teuer

Front Back

Transparent-whitish circular in the middle.

Cibicidoides wuellerstorfi

transparent white/yellowish

Other spicis found too!

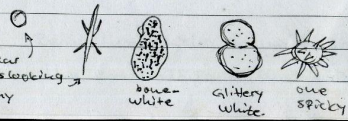

circular glass looking Shiny

bone-white

Glittery white

one spicky

24/1-2022

Sample 2:

A016-8-GC Mis5 37-38 cm Sec1 0.325m

Shive: 63-125 µm for T. quin.

(Too Few (0: 63-150 µm)) 150-250 µm for N. Pachy (17 st.) 63-250 µm for Benthic, 2 types

Nr. of forams: - No C. well found, T. quin: 140, 140, 140 (20st)

N. Pachy: 48, 51, 47 O.U: 0.053ug

Spicies picked: T. quinqueloba and N. Pachyderma

To few for one repeat! → O. Umbonatus

Observation: C. wuell are not found, smaller O. umb are few. T. quinqueloba & N. Pachyderma are more abundant! Lots of some quartz grains and also other creatures like radiolarians.

whitish transparent

← Transparent/glassy



some forams had been affected by chemical reactions giving them a golden colour → Not picked!

The abundance of quartz is due the interglacials! deposited during/due glaciers

Repeated 3 times.

Sample 3:

A06-8-GC HiSll 125-127 cm Sec 2

Shive: Benthic (C.wuell & O.umbo) 63-250 µm
T.egelida 63-125 µm

Nr. forams: T.egelida 95 (+15), 110, 110
O.umbo. Few found

weight: C.wuell. 0.24mg 0.2mg 0.25 mg

observation: When shieving T.egelida was mostly found in the smaller range 63 µm. The few bigger egelidas often harmed/broken (125 µm) or covered in muddy brownish-golden glitter. They often appear as very lumpy mud grains. Quartz is abundant, but also yellowish (dark orange-light) grains (minerals). The dirt covered / and very broken forams aren't picked!

other spicies found:
+ 7 T.quin found
+ 7 N.pachy found
+ 18 benthic

+50 Stetsonia horvathi

Repeated X3

T.egelida

Nice wall texture! Small in size with big opening and a lip on the first biggest chamber. The backside looks bloby like a N.Pachy but the front shape reminds of a T.quin. Usually 5 chambers and the colour is White. The apacus is on the side of the chamber

N.Pachy is more bloby rounded and has a cross. Nice opening with a lip. Usually 4 chambers. Wild calcification. Usually big ones!

T. quin usually Transparent/shiny, the final-chamber has a nice drop-shape going inwards to the inbillicus. Usually smaller holoden opening. A small foram!

other species found:

Benthic

Huge ~250 µm white shell, pointing out.

Transparent yellow brown-goldy looking. small!

A016-10PC Sec 1 11-12 cm ← closest cans no younger available.
Sample 1: Modern

Forams: Tever, C.wuell, O.umbo, N.Pachy

Shive: Benthic 63-250
N.Pachy 150-250

weight: C.wuell: 0.107mg → with the broken one 0.18 mg
O.umbo: 0.126 mg

nr. forams: N.Pachy (34 needed + 16 extra), 50, 50, 50

observations: General view, more quartz compared to forams. other species are few. Material looks clean. N.Pachy are the dominant foram, few benthics found. Good preservation of forams. Not enough benthic for 3 repeat (x1). Hopfull for 1.

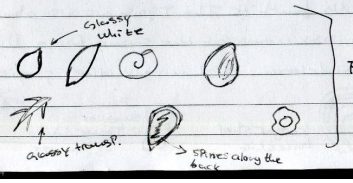

A016-10PC-Sec2 21-22 cm 16/2-2022

Sampel 2: MIS5

Forams: N.Pachy, C.wuell, O.Tener/umbo
T.quin

Shive: Benthic 63-250 µm
N.Pachy 150-250 µm
T.quin 63-125 µm

weight: C.wuell: 0,05 mg

Nr. forams.: N.Pachy (34 needed), 50, 50, 50
T.quin (125 needed) 125 +30, 125 +30, 125 +30
C.well x2

Observations: N.Pachy are more abundant than quartz. The N.Pachy usualy have dirt in the aparcher, could be pyrite or clay. otherwise they look clean and are well preserved. Few-No benthics. The T.quin are also very abundant easy to pick many at the same time. Nicly preserved and clean. Not many other species!

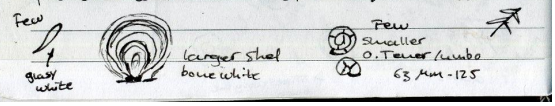


A016-10PC Sec 3 10-11 cm 16/2-2022

Sampel 3: MIS11

Forams: T.egelida, C.wuell, O.umbo/Tener

Shive: Benthic 63-250 µm
T.egelida 63-125 µm

weight: C.wuell 0.02 mg

nr. forams.: T.egelida (95 needed +30 extra) 125, 125, 125
C.wuell 9
O.umbo —

Observations: More quartz compared to forams. The C.wuell are white compared to the ones in previous sampels. They are also a little more rounded than flat. The benthics are few. T.egelidas are ok abundant. Not much of other species. Few bigger N.Pachys found!

Few C.wuell found. whiter than the ones usually seen. 23/2-2022 (Pic taken)
150 µm - 63 µm

Daniella has been picking from these sampels!

white, thin and long

white nut looking.

large white cup shel.
Transparentish → blurry colored glassy spike

Braided benthic.

large white worm looking.


circular white polished specie. The sides that are sticked together whith the other side is a bit flatten, giving it a disk look arround the blob.
Some 250 µm

212 µm N.Pachy found → Some/few

T.egelida-looking whit three chambers. Take them out.